

# An efficient implementable inexact entropic proximal point algorithm for a class of linear programming problems

Hong T. M. Chu\*, Ling Liang†, Kim-Chuan Toh‡ and Lei Yang§

May 29, 2022

## Abstract

We introduce a class of specially structured linear programming (LP) problems, which has favorable modeling capability for important application problems in different areas such as optimal transport, discrete tomography and economics. To solve these generally large-scale LP problems efficiently, we design an implementable inexact entropic proximal point algorithm (iEPPA) combined with an easy-to-implement dual block coordinate descent method as a subsolver. Unlike existing entropy-type proximal point algorithms, our iEPPA employs a more practically checkable stopping condition for solving the associated subproblems while achieving provable convergence. Moreover, when solving the capacity constrained multi-marginal optimal transport (CMOT) problem (a special case of our LP problem), our iEPPA is able to bypass the underlying numerical instability issues that often appear in the popular entropic regularization approach, since our algorithm does not require the proximal parameter to be very small in order to obtain an accurate approximate solution. Numerous numerical experiments show that our iEPPA is highly efficient and robust for solving large-scale CMOT problems, in comparison to the (stabilized) Dykstra’s algorithm and the commercial solver Gurobi. Moreover, the experiments on discrete tomography also highlight the potential modeling power of our model.

**Keywords:** Linear programming; proximal point algorithm; entropic proximal term; block coordinate descent; capacity constrained multi-marginal optimal transport.

## 1 Introduction

In this paper, we introduce a class of specially structured linear programming (LP) problems with the following form:

$$\begin{aligned} \min \quad & \langle C, X \rangle \\ \text{s.t.} \quad & X \in \Omega := \left\{ X \in \mathbb{R}^{n_1 \times n_2 \times n_3} : \mathcal{A}^{(i)}(X) = \mathbf{b}^{(i)}, \quad i = 1, \dots, N, \quad 0 \leq X \leq U \right\}, \end{aligned} \quad (1.1)$$

where  $\langle \cdot, \cdot \rangle$  denotes the standard inner product in  $\mathbb{R}^{n_1 \times n_2 \times n_3}$ ,  $\mathcal{A}^{(i)} : \mathbb{R}^{n_1 \times n_2 \times n_3} \rightarrow \mathbb{R}^{m_i}$  is a given linear mapping defined by

$$\mathcal{A}^{(i)}(X) := \begin{bmatrix} \langle A_1^{(i)}, X \rangle \\ \vdots \\ \langle A_{m_i}^{(i)}, X \rangle \end{bmatrix}, \quad A_j^{(i)} \in \mathbb{R}^{n_1 \times n_2 \times n_3}, \quad 1 \leq j \leq m_i, \quad 1 \leq i \leq N,$$

\*Department of Mathematics, National University of Singapore ([hongtmchu@nus.edu](mailto:hongtmchu@nus.edu)).

†Department of Mathematics, National University of Singapore ([liang.ling@nus.edu](mailto:liang.ling@nus.edu)).

‡Department of Mathematics, and Institute of Operations Research and Analytics, National University of Singapore ([mattohkc@nus.edu.sg](mailto:mattohkc@nus.edu.sg)). This research is supported in part by the Ministry of Education of Singapore under Academic Research Fund Grant number: MOE2019-T3-1-010.

§(Corresponding author) Department of Mathematics, National University of Singapore ([matylei@nus.edu.sg](mailto:matylei@nus.edu.sg)).

$\mathbf{b}^{(i)} = (b_1^{(i)}, \dots, b_{m_i}^{(i)})^\top \in \mathbb{R}^{m_i}$  ( $i = 1, \dots, N$ ),  $C \in \mathbb{R}^{n_1 \times n_2 \times n_3}$  and  $U \in \mathbb{R}_{++}^{n_1 \times n_2 \times n_3} \cup \{\infty\}^{n_1 \times n_2 \times n_3}$  are given data. Moreover, the linear mappings  $\mathcal{A}^{(i)}$  ( $i = 1, \dots, N$ ) satisfy the following assumption.

**Assumption 1.** For each  $1 \leq i \leq N$ ,  $A_j^{(i)}$  only has binary entries (0 or 1) for  $j = 1, \dots, m_i$ , and the given constraint tensors  $\{A_j^{(i)} \mid j = 1, \dots, m_i\}$  satisfy the property that

$$A_j^{(i)} \circ A_k^{(i)} = 0, \quad \text{if } j \neq k, j, k = 1, \dots, m_i,$$

where “ $\circ$ ” denotes the Hadamard product. The above property is equivalent to saying that the non-zero patterns of any two distinct constraint tensors  $A_j^{(i)}$  and  $A_k^{(i)}$  do not overlap in the  $i$ -block of the linear constraints  $\mathcal{A}^{(i)}(X) = \mathbf{b}^{(i)}$ .

The desired structures imposed on  $\mathcal{A}^{(i)}$  ( $i = 1, \dots, N$ ) in Assumption 1 may look unusual at the first glance, but such structures do appear in important applications in various areas (see the following example and those in Section 2). As we shall see later, such special structures allow us to design a highly efficient algorithm to solve the corresponding LPs since they can greatly facilitate the computations of the subproblems involved in our algorithm (see Section 4 and Appendix A for more details). One representative problem that can be modeled by (1.1) is the discrete 3-dimensional capacity constrained multi-marginal optimal transport (CMOT) problem with

$$\begin{aligned} A_j^{(1)} &= \mathbf{e}_j^{(1)} \otimes \mathbf{1}_{n_2} \otimes \mathbf{1}_{n_3}, \quad j = 1, \dots, n_1, \\ A_j^{(2)} &= \mathbf{1}_{n_1} \otimes \mathbf{e}_j^{(2)} \otimes \mathbf{1}_{n_3}, \quad j = 1, \dots, n_2, \\ A_j^{(3)} &= \mathbf{1}_{n_1} \otimes \mathbf{1}_{n_2} \otimes \mathbf{e}_j^{(3)}, \quad j = 1, \dots, n_3, \end{aligned} \tag{1.2}$$

where  $\mathbf{e}_j^{(i)}$  denotes the  $j$ th unit vector in  $\mathbb{R}^{n_i}$  ( $i = 1, 2, 3$ ),  $\mathbf{1}_{n_i}$  denotes the  $n_i$ -dimensional vector of all ones for  $i = 1, 2, 3$ , and “ $\otimes$ ” denotes the tensor product (see the definition at the end of this section). Specifically, with these linear mappings, problem (1.1) reduces to

$$\begin{aligned} \min_{X \in \mathbb{R}^{n_1 \times n_2 \times n_3}} \quad & \langle C, X \rangle \\ \text{s.t.} \quad & \sum_{s,t} X_{rst} = a_r, \quad r = 1, \dots, n_1, \quad \sum_{r,t} X_{rst} = b_s, \quad s = 1, \dots, n_2, \\ & \sum_{r,s} X_{rst} = c_t, \quad t = 1, \dots, n_3, \quad 0 \leq X \leq U, \end{aligned} \tag{1.3}$$

where  $\mathbf{a} := (a_1, \dots, a_{n_1})^\top \in \Sigma_{n_1}$ ,  $\mathbf{b} := (b_1, \dots, b_{n_2})^\top \in \Sigma_{n_2}$ ,  $\mathbf{c} := (c_1, \dots, c_{n_3})^\top \in \Sigma_{n_3}$ , with  $\Sigma_{n_i}$  denoting the  $n_i$ -dimensional unit simplex for  $i = 1, 2, 3$ . In this case,  $\mathbf{a}$ ,  $\mathbf{b}$  and  $\mathbf{c}$  are also called the marginals. Problem (1.3) was first proposed and studied by Korman and McCann [22, 23] in the 2-marginal continuous case as an important variant of the classical 2-marginal optimal transport (OT) problem. This variant takes into account the limitations of transport capacity on the coupling weights<sup>1</sup> via imposing a proper upper bound constraint  $X \leq U$ , and hence it is able to better model some real-life situations. Besides the CMOT problem described above, our model (1.1) is also able to handle many other application problems, for example, discrete tomography [1, 7, 38], disaggregation of industry-by-industry input-output tables in economics [19], and reconstructions of unknown inter-bank liabilities with fixed constraints [17]. More details will be provided in Section 2.

Note that problem (1.1) has  $n_1 n_2 n_3$  nonnegative variables and  $\sum_{i=1}^N m_i$  linear equality constraints, and thus it is usually a very large-scale LP when the dimension of the variable or the number of blocks of linear constraints is large. Therefore, classical LP methods such as the simplex method and the interior point method may no longer be efficient enough or may consume too much memory when solving this problem. Recently, an entropic regularized approach has been proposed in [6] to **approximately** solve problem (1.3) in the 2-marginal case with impressive numerical performance. This approach basically modifies the original LP problem by adding an entropic regularization to the objective, and then applies

<sup>1</sup>This consideration can date back to [24], and possibly earlier.

a certain efficient first-order method to solve the resulting computationally more tractable regularized problem to obtain an approximate solution of the original LP problem. In [6], the Dykstra’s algorithm<sup>2</sup> with Kullback-Leibler projections (DyKL) is adapted to solve the entropic regularized counterpart of problem (1.3) in the 2-marginal case (see (B.1)). This algorithm can be highly efficient if a crude approximate solution is adequate, in which case the regularization parameter is not required to be a very small value. To obtain a more accurate solution, one must decrease the regularization parameter to a small value. However, when the regularization parameter is small, just like the Sinkhorn’s algorithm [33] adapted in [12] for approximately solving the classical 2-marginal OT problem, DyKL also encounters the same difficulties of numerical instabilities (due to loss of accuracy involving overflow/underflow operations) and slow convergence speed. Though the former difficulty can partially be alleviated by some stabilization techniques (e.g., the *log-sum-exp* operation [28, Section 4.4]) at the expense of losing some computational efficiency, the latter difficulty of slow convergence, however, is unavoidable when the regularization parameter is small, as clearly observed from our numerical experiments in Section 5. In addition, we are not aware of fast algorithms that are specifically designed for solving the more general problem (1.1).

In this paper, we develop an implementable inexact entropic proximal point algorithm (iEPPA) for problem (1.1), which solves the original LP problem faithfully via approximately solving a sequence of subproblems (3.2), each involving a special entropic proximal term. Our iEPPA falls into the family of Bregman-distance-based PPA [10, 11, 14, 15] and the family of  $\phi$ -divergence-based PPA [3, 16, 20, 21, 34, 35], both of which have been widely studied in the literature. However, we should point out that we have made an essential change to the algorithm by introducing a more practically implementable stopping condition (3.3) for solving the subproblems involved. Thus, existing convergence results may not be applicable and the convergence analysis has to be re-established for our iEPPA; see Theorem 1. Moreover, as a byproduct, we actually develop a unified inexact framework for EPPA including Teboulle’s framework [35] and Eckstein’s framework [15] as special cases. This makes our iEPPA more flexible to fit different scenarios. To solve the subproblem (3.2) in iEPPA, we derive its dual problem and characterize the properties of its optimal solutions in Section 4. The resulting dual problem is a convex optimization problem with  $N + 1$  separable blocks of variables and hence is conceivably more tractable. We then apply a block coordinate descent (BCD) method to solve it and establish the linear convergence by revisiting some classical results for BCD in [25, 26, 37]. We also show how the subproblems involved in the BCD method can be efficiently solved exactly. Moreover, we emphasize that no stabilization technique is needed for each BCD update since our iEPPA generally does not require a small proximal parameter in each iteration. This is indeed a key advantage of our iEPPA over the popular entropic regularization approach in [6]. Recently, a similar algorithmic framework studied by Eckstein [15] was also adapted in [39] for solving the classical OT problem with encouraging numerical performance. However, the algorithm there was developed under a rather stringent inexact condition, which is nontrivial to verify *or* implement in practice.

The contributions of this paper are summarized as follows.

1. We introduce a class of specially structured LP problems (1.1), which covers some important existing problems and has favorable modeling capability; see Section 2. For example, it is able to formulate a tomography problem *without* using a high-order tensor. This is in sharp contrast to [1, 7] where a high-order tensor (with its order equals to two plus the number of projection directions) is used to model a 2D tomography problem, and consequently the resulting problem is extremely large-scale and is prohibitively expensive to solve in terms of both memory consumption and computational cost.
2. We develop an efficient iEPPA combined with a dual BCD method, namely, iEPPA+BCD, to solve the proposed structured LP problem (1.1). It has the important strength of being able to faithfully solve the original problem *without* requiring the proximal parameter to be very small.

---

<sup>2</sup>More details on the Dykstra’s algorithm and its Bregman extension can be found in [5, 13].

As a result, when solving the CMOT problem (1.3), it can bypass the inherent numerical instabilities that often plague the entropic regularization approach. While our iEPPA+BCD framework is not completely new but a novel combination of existing algorithms in the optimization literature, we have nevertheless introduced an essential modification to make the algorithm practically implementable by proposing a computationally checkable stopping condition for finding a sufficiently accurate approximate solution of the subproblem in each iEPPA iteration to ensure the convergence of the overall algorithm.

3. We conduct rigorous numerical experiments to illustrate the efficiency of our iEPPA+BCD framework for solving the CMOT problem (1.3), compared to the DyKL and the powerful commercial solver Gurobi. Our computational results for 2-marginal and 3-marginal CMOT on synthetic data demonstrate that our iEPPA+BCD framework is highly efficient and robust. The experiments on discrete tomography also highlight the modeling power of our model.

Finally, we mention that setting the decision variable  $X$  to be a third-order tensor in problem (1.1) is only for the ease of presentation. All results and algorithms developed in this paper can be extended straightforwardly to the matrix case or the higher order tensor case.

The rest of this paper is organized as follows. We present details on the modeling power of problem (1.1) in Section 2. The iEPPA for solving (1.1) and its convergence results are described in Section 3. The dual BCD method for solving the subproblem and its convergence analysis are presented in Section 4. Moreover, the details on the implementable verification of our new inexact condition is also included in Section 4. Extensive numerical results are reported in Section 5, with some concluding remarks given in Section 6.

**Notation and Preliminaries** In this paper, the elements of a third-order tensor  $X \in \mathbb{R}^{n_1 \times n_2 \times n_3}$  are denoted as  $X_{rst}$  where  $1 \leq r \leq n_1$ ,  $1 \leq s \leq n_2$ ,  $1 \leq t \leq n_3$ . For any tensors  $X, Y \in \mathbb{R}^{n_1 \times n_2 \times n_3}$ , we define their inner product as  $\langle X, Y \rangle := \sum_{r=1}^{n_1} \sum_{s=1}^{n_2} \sum_{t=1}^{n_3} X_{rst} Y_{rst}$ . Then, the corresponding Fröbenius norm of  $X$  is defined by  $\|X\|_F := \sqrt{\langle X, X \rangle}$ . For any  $X, Y \in \mathbb{R}^{n_1 \times n_2 \times n_3}$ , the Hadamard product of  $X$  and  $Y$  is defined by

$$(X \circ Y)_{rst} := X_{rst} Y_{rst}, \quad 1 \leq r \leq n_1, 1 \leq s \leq n_2, 1 \leq t \leq n_3.$$

Similarly, we use “./” to denote the element-wise division operator. We also use “ $\otimes$ ” to denote the tensor product of vectors. In particular, let  $\mathbf{u}^{(i)} \in \mathbb{R}^{n_i}$  ( $i = 1, 2, 3$ ) be three arbitrary column vectors. Their tensor product is denoted by  $\mathbf{u}^{(1)} \otimes \mathbf{u}^{(2)} \otimes \mathbf{u}^{(3)} \in \mathbb{R}^{n_1 \times n_2 \times n_3}$  whose elements are given by

$$(\mathbf{u}^{(1)} \otimes \mathbf{u}^{(2)} \otimes \mathbf{u}^{(3)})_{rst} := u_r^{(1)} u_s^{(2)} u_t^{(3)}, \quad 1 \leq r \leq n_1, 1 \leq s \leq n_2, 1 \leq t \leq n_3.$$

Let  $\mathbb{E}$  be a finitely dimensional real Euclidean space equipped with an inner product  $\langle \cdot, \cdot \rangle$  and its induced norm  $\|\cdot\|$ . For an extended-real-valued function  $f : \mathbb{E} \rightarrow [-\infty, \infty]$ , we say that it is *proper* if  $f(\mathbf{x}) > -\infty$  for all  $\mathbf{x} \in \mathbb{E}$  and its domain  $\text{dom } f := \{\mathbf{x} \in \mathbb{E} : f(\mathbf{x}) < \infty\}$  is nonempty. A proper function  $f$  is said to be closed if it is lower semicontinuous. Assume that  $f : \mathbb{E} \rightarrow (-\infty, \infty]$  is a proper closed convex function. For a given  $\nu \geq 0$ , the  $\nu$ -subdifferential of  $f$  at  $\mathbf{x} \in \text{dom } f$  is defined by  $\partial_\nu f(\mathbf{x}) := \{\mathbf{d} \in \mathbb{E} : f(\mathbf{y}) \geq f(\mathbf{x}) + \langle \mathbf{d}, \mathbf{y} - \mathbf{x} \rangle - \nu, \forall \mathbf{y} \in \mathbb{E}\}$  and its conjugate function  $f^* : \mathbb{E} \rightarrow (-\infty, \infty]$  is defined by  $f^*(\mathbf{y}) := \sup\{\langle \mathbf{y}, \mathbf{x} \rangle - f(\mathbf{x}) : \mathbf{x} \in \mathbb{E}\}$ . For any  $\mathbf{x}, \mathbf{y} \in \mathbb{E}$ , it follows from [30, Theorem 23.5] that

$$\mathbf{y} \in \partial f(\mathbf{x}) \iff \mathbf{x} \in \partial f^*(\mathbf{y}). \quad (1.4)$$

Moreover, we call a proper closed convex function  $f$  essentially smooth if (i) the interior of  $\text{dom } f$ , denoted by  $\text{int dom } f$ , is not empty; (ii)  $f$  is differentiable on  $\text{int dom } f$ ; (iii)  $\|\nabla f(x_k)\| \rightarrow \infty$  for every sequence  $\{x_k\}$  in  $\text{int dom } f$  converging to a boundary point of  $\text{int dom } f$ ; see [30, page 251].

We also recall two types of linear convergence, which will be used in our convergence analysis; more details can be found in [27, Appendix A.2]. A sequence  $\{a_k\}$  is said to be Q-linearly convergent to  $a^*$  if

there exist  $\rho \in (0, 1)$  and  $k_0 \geq 1$  such that  $\|a^{k+1} - a^*\| \leq \rho \|a^k - a^*\|$  for all  $k \geq k_0$ . A sequence  $\{b_k\}$  is said to be R-linearly convergent to  $b^*$  if there exists a nonnegative sequence  $\{a_k\}$  such that  $\|b_k - b^*\| \leq a_k$  for all  $k$  and  $\{a_k\}$  is Q-linearly convergent to zero.

Finally, we make a blanket feasibility assumption for problem (1.1) throughout this paper.

**Assumption 2.** *The set  $\Omega \cap \mathbb{R}_{++}^{n_1 \times n_2 \times n_3}$  is nonempty.*

Assumption 2 is used to guarantee the well-definedness of problem (1.1) and our iEPPA in Algorithm 1 presented in the next section. Indeed, the nonemptiness of the set  $\Omega \cap \mathbb{R}_{++}^{n_1 \times n_2 \times n_3}$  implies that  $\Omega$  is nonempty. Since  $\Omega$  is also closed and bounded, then problem (1.1) has at least one optimal solution.

## 2 Modeling power of problem (1.1)

Recall that problem (1.1) can naturally model the CMOT problem (1.3). In this section, we further demonstrate the potential modeling capability of problem (1.1) by showing that it can provide a unified framework to model some other important real-world applications.

In the 2-dimensional discrete tomography problem studied in [38], one is given the marginals obtained from an  $n \times n$  matrix (for simplicity, we discuss the case of a matrix instead of a third-order tensor) by summing its entries along different directions, for example,  $0^\circ$ ,  $45^\circ$ ,  $90^\circ$  and  $135^\circ$  directions. In this case, the formulation in [1] would require a sixth-order tensor to model the problem as a 6-marginal optimal transport problem. Unfortunately, this approach leads to an exponential increase in the computational cost because of the curse of dimensionality brought about by the extra dimensions introduced in the higher-order tensor. But using our model in (1.1), the variable remains as a matrix and the projections along four directions are formulated as four blocks of linear constraints, each represented by a linear mapping  $\mathcal{A}^{(i)}(X) = \mathbf{b}^{(i)}$  with  $\mathbf{b}^{(i)}$  being the given  $i$ th marginal for  $i = 1, \dots, 4$ . More specifically, let  $\mathbf{1}_n$  and  $\mathbf{e}_j$  be the vector of all ones and the  $j$ -th standard unit vector in  $\mathbb{R}^n$ , respectively. We set

$$\begin{aligned} A_j^{(1)} &= \mathbf{e}_j \mathbf{1}_n^\top, \quad j = 1, \dots, n, & A_j^{(3)} &= \mathbf{1}_n \mathbf{e}_j^\top, \quad j = 1, \dots, n, \\ A_j^{(2)} &= \text{hankel}(\mathbf{e}_j, \mathbf{0}_n), \quad j = 1, \dots, n, & A_{j+n}^{(2)} &= \text{hankel}(\mathbf{0}_n, \mathbf{e}_j), \quad j = 1, \dots, n-1, \\ A_j^{(4)} &= \text{toeplitz}(\mathbf{e}_j, \mathbf{0}_n), \quad j = 1, \dots, n, & A_{j+n}^{(4)} &= \text{toeplitz}(\mathbf{0}_n, \mathbf{e}_{j+1}), \quad j = 1, \dots, n-1, \end{aligned} \tag{2.1}$$

where we have used MATLAB commands for generating Toeplitz and Hankel matrices. For this example, one can easily check that the constraint matrices associated with each linear mapping  $\mathcal{A}^{(i)}$  satisfy Assumption 1. More details will be presented in our numerical experiments in subsection 5.3.

In constructing an unknown 2-dimensional industry-by-industry input-output table in a nation's annual economy, one may also be interested in the corresponding tables of different regions *or* of different quarters. The constraints in such a problem are similar to those of the standard CMOT problem, but the objective function is the cross-entropy  $\sum_{rst} X_{rst} \log(X_{rst}/\bar{X}_{rst})$  between the estimated tensor  $X$  and a given prior  $\bar{X}$  that may have been constructed in the past. In [19], the authors proposed to work with a multi-dimensional table to accommodate the disaggregation of the input-output table, where the additional dimension can represent geographical regions *or* quarters. They also proposed a multi-dimensional RAS method which extends the classical RAS method (equivalent to the Sinkhorn's algorithm) to solve the corresponding multi-dimensional cross-entropy model that minimizes an entropy based objective function subject to given multi-marginal constraints. However, it is unclear how the multi-dimensional RAS method can be used to solve an extension of the model when some entries of the input-output table are given. The power of our model (1.1) lies in the fact that it can be employed to disaggregate an input-output table while incorporating partially given information on some parts of the input-output table. Moreover, our proposed iEPPA for solving problem (1.1) can also be modified straightforwardly to solve the extended disaggregation problem.

In [17], the authors studied the problem of estimating inter-bank liabilities given the row and column aggregates of the liabilities of the banks. The problem is to reconstruct the bank-by-bank table given the total liabilities of the rows and columns. The aforementioned paper proposed a Bayesian method for

minimizing the KL-divergence of the estimated matrix from a pre-specified input matrix. It allows the model to incorporate fixed known liabilities among some of the banks. In particular, since a bank does not have any liability to itself, the main diagonal entries of the matrix are fixed to be zero. Here again, our model (1.1) can easily accommodate such kinds of side constraints. For example, to fix the main diagonal of a matrix  $X \in \mathbb{R}^{n \times n}$  to be zero, we just need to add a block of constraints, say the  $i$ -th block  $\mathcal{A}^{(i)}(X) = \mathbf{b}^{(i)}$ , such that  $A_j^{(i)} = \mathbf{e}_j \mathbf{e}_j^\top$  for  $j = 1, \dots, n$ , and  $\mathbf{b}^{(i)} = \mathbf{0}$ . In this case, it is easy to check that the constraint matrices  $\{A_j^{(i)} \mid j = 1, \dots, n\}$  do satisfy Assumption 1. More generally, when the total liability of the banks in a country to all other banks within the same country is known (such data may be collected by the country's central bank), such information can be incorporated into the reconstruction problem by using our model. Specifically, we can add the constraints  $\mathcal{A}^{(i)}(X) = \mathbf{b}^{(i)}$  such that for the  $j$ -th country, the constraint matrix  $A_j^{(i)}$  has a submatrix of all ones (assuming that the banks in a country are placed contiguously) at the positions corresponding to the country's banks, while all the other entries are zero.

### 3 An implementable inexact entropic proximal point algorithm

In this section, we develop an implementable inexact entropic proximal point algorithm (iEPPA) for solving problem (1.1). To describe the iterates of the iEPPA, we first rewrite problem (1.1) as follows:

$$\min_X \delta_{\Omega^\circ}(X) + \langle C, X \rangle, \quad \text{s.t. } X \geq 0, \quad (3.1)$$

where  $\delta_{\Omega^\circ}(\cdot)$  is the indicator function of the set  $\Omega^\circ$  defined as

$$\Omega^\circ := \{X \in \mathbb{R}^{n_1 \times n_2 \times n_3} : \mathcal{A}^{(i)}(X) = \mathbf{b}^{(i)}, i = 1, \dots, N, X \leq U\}.$$

Obviously, the set  $\Omega^\circ$  is formed by removing the non-negative constraint on  $X$  from the set  $\Omega$  and hence  $\Omega \subseteq \Omega^\circ$ . We also introduce the Bregman distance [8] associated with the Boltzmann-Shannon entropy function  $\phi(X) = \sum_{rst} X_{rst} \log X_{rst} - X_{rst}$  as follows:

$$\mathcal{D}_\phi(X, Y) := \phi(X) - \phi(Y) - \langle \nabla \phi(Y), X - Y \rangle, \quad \forall X \in \mathbb{R}_{++}^{n_1 \times n_2 \times n_3}, Y \in \mathbb{R}_{++}^{n_1 \times n_2 \times n_3}.$$

It is easy to see that  $\mathcal{D}_\phi(X, Y) \geq 0$  and the equality holds if and only if  $X = Y$ . Then, the iEPPA for solving (3.1) (hence (1.1)) is presented as Algorithm 1.

---

**Algorithm 1** An implementable inexact entropic proximal point algorithm (iEPPA) for solving (3.1)

---

**Input:** Let  $\{\varepsilon_k\}_{k=0}^\infty$ ,  $\{\nu_k\}_{k=0}^\infty$ ,  $\{\eta_k\}_{k=0}^\infty$  and  $\{\mu_k\}_{k=0}^\infty$  be four sequences of nonnegative scalars. Choose  $X^0 = \tilde{X}^0 \in \mathbb{R}_{++}^{n_1 \times n_2 \times n_3}$  arbitrarily. Set  $k = 0$ .

**while** the termination criterion is not met, **do**

**Step 1.** Find a pair  $(X^{k+1}, \tilde{X}^{k+1})$  by approximately solving the following problem

$$\min_X \delta_{\Omega^\circ}(X) + \langle C, X \rangle + \varepsilon_k \mathcal{D}_\phi(X, X^k), \quad (3.2)$$

such that  $X^{k+1} \in \mathbb{R}_{++}^{n_1 \times n_2 \times n_3}$ ,  $\tilde{X}^{k+1} \in \Omega$  and

$$\begin{aligned} \Delta^k &\in \partial_{\nu_k} \delta_{\Omega^\circ}(\tilde{X}^{k+1}) + C + \varepsilon_k (\nabla \phi(X^{k+1}) - \nabla \phi(X^k)) \\ \text{with } \|\Delta^k\|_F &\leq \eta_k, \quad \mathcal{D}_\phi(\tilde{X}^{k+1}, X^{k+1}) \leq \mu_k. \end{aligned} \quad (3.3)$$

**Step 2.** Set  $k = k + 1$  and go to **Step 1**.

**end while**

**Output:**  $(X^k, \tilde{X}^k)$

---

The reader may have observed that the iEPPA in Algorithm 1 basically solves the original problem (3.1) (hence (1.1)) via approximately solving a sequence of subproblems (3.2) each involving a special entropic Bregman proximal term. Note that the Boltzmann-Shannon entropy function  $\phi(X) = \sum_{rst} X_{rst} \log X_{rst} - X_{rst}$  is essentially smooth and strictly convex on  $\mathbb{R}_+^{n_1 \times n_2 \times n_3}$ . This together with Assumption 2 ensure that each subproblem (3.2) is well-defined in the sense that its optimal solution (denoted by  $X^{k,*}$ ) uniquely exists and lies in  $\mathbb{R}_{++}^{n_1 \times n_2 \times n_3}$ . Specifically, since  $\Omega^\circ \cap \text{dom } \phi = \Omega$  is bounded, the objective function in subproblem (3.2) is level-bounded. Thus, a solution exists [31, Theorem 1.9] and must be unique since  $\phi$  is strictly convex. The essential smoothness of  $\phi$  and Assumption 2 further imply that  $X^{k,*}$  can only lie in  $\mathbb{R}_{++}^{n_1 \times n_2 \times n_3}$ . Obviously, our inexact condition (3.3) always holds when  $X^{k+1} = \tilde{X}^{k+1} = X^{k,*}$  and hence it is also well-defined.

The inexact condition (3.3) is quite flexible for covering many existing inexact conditions, and more importantly, it makes our iEPPA more practical for solving (3.1) (hence (1.1)). Specifically, when  $\nu_k \equiv \eta_k \equiv \mu_k \equiv 0$ ,  $X^{k+1}$  (equals to  $\tilde{X}^{k+1}$ ) must be the exact optimal solution of subproblem (3.2). In this case, our iEPPA reduces to the classical exact generalized PPA such as the  $\phi$ -divergence-based PPA [3, 16, 20, 21, 34] and the Bregman-distance-based PPA [10, 11, 14]. When  $\eta_k \equiv \mu_k \equiv 0$ , condition (3.3) reduces to

$$0 \in \partial_{\nu_k} \delta_{\Omega^\circ}(X^{k+1}) + C + \varepsilon_k (\nabla \phi(X^{k+1}) - \nabla \phi(X^k)), \quad (3.4)$$

which is considered by Teboulle [35] in the  $\phi$ -divergence-based PPA that allows the approximate computations of the subdifferential of  $\delta_{\Omega^\circ}$  at  $X^{k+1}$ , provided  $X^{k+1} \in \Omega^\circ$ . When  $\nu_k \equiv \mu_k \equiv 0$ , condition (3.3) reduces to

$$\Delta^k \in \partial \delta_{\Omega^\circ}(X^{k+1}) + C + \varepsilon_k (\nabla \phi(X^{k+1}) - \nabla \phi(X^k)) \quad \text{with } \|\Delta^k\|_F \leq \eta_k, \quad (3.5)$$

which is considered by Eckstein [15] in the Bregman-distance-based PPA and is typically easier to check than the  $\nu$ -subdifferential-based condition (3.4). But again, it requires  $X^{k+1}$  to be in  $\Omega^\circ$ . This inexact algorithmic framework has also been adapted in [39] for solving the classical 2-marginal OT problem. However, we should mention that *neither* Teboulle's inexact condition (3.4) *nor* Eckstein's inexact condition (3.5) is easily implementable and practical for solving the subproblem with the complicated constraint that  $X \in \Omega^\circ$ . This is because it is nontrivial to find a point  $X^{k+1}$  that *simultaneously* satisfies  $X^{k+1} \in \Omega^\circ$  (required by the nonemptiness of  $\partial_{\nu_k} \delta_{\Omega^\circ}(X^{k+1})$  or  $\partial \delta_{\Omega^\circ}(X^{k+1})$ ) and  $X^{k+1} \in \mathbb{R}_{++}^{n_1 \times n_2 \times n_3}$  (required by the essentially smoothness of  $\phi$ ). The aforementioned inadequacy thus motivated us to further relax conditions (3.4) and (3.5) to condition (3.3), in which  $\partial_{\nu_k} \delta_{\Omega^\circ}$  and  $\nabla \phi$  are allowed to be computed at two slightly different points, respectively. We shall show later in subsection 4.2 that the verification of our inexact condition (3.3) is more practically implementable.

By some simple manipulations, one can see that the subproblem (3.2) with the linear mappings defined in (1.2) actually has the same form as the entropic regularized counterpart of the capacity constrained optimal transport problem considered in [6, Section 5.2]. However, in both theory and practice, the proximal parameter  $\varepsilon_k$  involved in our iEPPA does not need to take a very small value to obtain an accurate solution of the original problem (3.1) (hence (1.1)). This is undoubtedly an important advantage for our approach to avoid some inherent numerical issues that often appear in the entropic regularization approach.

We next establish the convergence of our iEPPA in Algorithm 1. Our analysis is inspired by several existing works (see, for example, [15, 35]), but is much more involved due to the more flexible inexact condition (3.3). We shall start with some elementary preliminaries. It is known from [9, Section 6.1] that the Boltzmann-Shannon entropy function  $\phi$  has many elegant properties as a Bregman function (see [9, Definition 2.1]). We point out three of them below that are useful in our subsequential analysis. More details on the Bregman function can be found in [4, Section 4].

**Property 1.** *The following properties hold for  $\phi(X) = \sum_{rst} X_{rst} \log X_{rst} - X_{rst}$ .*

- (i) *For any  $X \in \mathbb{R}_+^{n_1 \times n_2 \times n_3}$ ,  $\mathcal{D}_\phi(X, \cdot)$  is level-bounded.*
- (ii) *If  $\{Y^k\} \subseteq \mathbb{R}_{++}^{n_1 \times n_2 \times n_3}$  converges to some  $Y^* \in \mathbb{R}_{++}^{n_1 \times n_2 \times n_3}$ , then  $\mathcal{D}_\phi(Y^*, Y^k) \rightarrow 0$ .*

(iii) (**Convergence consistency**) If  $\{X^k\} \subseteq \mathbb{R}_+^{n_1 \times n_2 \times n_3}$  and  $\{Y^k\} \subseteq \mathbb{R}_{++}^{n_1 \times n_2 \times n_3}$  are two sequences such that  $\{X^k\}$  is bounded,  $Y^k \rightarrow Y^*$  and  $\mathcal{D}_\phi(X^k, Y^k) \rightarrow 0$ , then  $X^k \rightarrow Y^*$ .

We also recall two well-known results.

**Lemma 1 (Three points identity [11, Lemma 3.1]).** For any  $X \in \mathbb{R}_+^{n_1 \times n_2 \times n_3}$  and  $Y, Z \in \mathbb{R}_{++}^{n_1 \times n_2 \times n_3}$ , the following identity holds:

$$\langle \nabla\phi(Y) - \nabla\phi(Z), X - Y \rangle = \mathcal{D}_\phi(X, Z) - \mathcal{D}_\phi(X, Y) - \mathcal{D}_\phi(Y, Z).$$

**Lemma 2 ([29, Section 2.2]).** Suppose that  $\{a_k\}_{k=0}^\infty \subseteq \mathbb{R}$  and  $\{\gamma_k\}_{k=0}^\infty \subseteq \mathbb{R}$  are two sequences such that  $\{a_k\}$  is bounded from below,  $\sum_{k=0}^\infty \gamma_k < \infty$ , and  $a_{k+1} \leq a_k + \gamma_k$  holds for all  $k$ . Then,  $\{a_k\}$  is convergent.

We are now ready to give the main convergence result.

**Theorem 1 (Convergence of the iEPPA).** Suppose that Assumption 2 holds and  $\{\varepsilon_k\}_{k=0}^\infty, \{\nu_k\}_{k=0}^\infty, \{\eta_k\}_{k=0}^\infty, \{\mu_k\}_{k=0}^\infty$  are four sequences of nonnegative scalars. Let  $\{X^k\}$  and  $\{\tilde{X}^k\}$  be the sequences generated by the iEPPA in Algorithm 1. If  $0 < \underline{\varepsilon} \leq \varepsilon_k \leq \bar{\varepsilon} < \infty$ ,  $\sum \nu_k < \infty$ ,  $\sum \eta_k < \infty$  and  $\sum \mu_k < \infty$ , then  $\{X^k\}$  and  $\{\tilde{X}^k\}$  converge to a same optimal solution of problem (3.1) (hence problem (1.1)).

*Proof.* First, for all  $X \in \Omega$ , since  $0 \leq X \leq U$ , then  $\|X\|_F \leq \rho := \|U\|_F$ . From condition (3.3), there exists a  $D^{k+1} \in \partial_{\nu_k} \delta_{\Omega^\circ}(\tilde{X}^{k+1})$  such that

$$\Delta^k = D^{k+1} + C + \varepsilon_k (\nabla\phi(X^{k+1}) - \nabla\phi(X^k)).$$

Then, for any  $P \in \Omega \subseteq \Omega^\circ$ , we see that

$$0 \geq \langle D^{k+1}, P - \tilde{X}^{k+1} \rangle - \nu_k = \langle \Delta^k - C - \varepsilon_k (\nabla\phi(X^{k+1}) - \nabla\phi(X^k)), P - \tilde{X}^{k+1} \rangle - \nu_k,$$

which implies that

$$\langle C, \tilde{X}^{k+1} \rangle \leq \langle C, P \rangle + \varepsilon_k \langle \nabla\phi(X^{k+1}) - \nabla\phi(X^k), P - \tilde{X}^{k+1} \rangle + \langle \Delta^k, \tilde{X}^{k+1} - P \rangle + \nu_k. \quad (3.6)$$

Note that

$$\begin{aligned} & \langle \nabla\phi(X^{k+1}) - \nabla\phi(X^k), P - \tilde{X}^{k+1} \rangle \\ &= \langle \nabla\phi(X^{k+1}) - \nabla\phi(X^k), P - X^{k+1} \rangle - \langle \nabla\phi(X^{k+1}) - \nabla\phi(X^k), \tilde{X}^{k+1} - X^{k+1} \rangle \\ &= \mathcal{D}_\phi(P, X^k) - \mathcal{D}_\phi(P, X^{k+1}) - \mathcal{D}_\phi(X^{k+1}, X^k) - (\mathcal{D}_\phi(\tilde{X}^{k+1}, X^k) - \mathcal{D}_\phi(\tilde{X}^{k+1}, X^{k+1}) - \mathcal{D}_\phi(X^{k+1}, X^k)) \\ &= \mathcal{D}_\phi(P, X^k) - \mathcal{D}_\phi(P, X^{k+1}) - \mathcal{D}_\phi(\tilde{X}^{k+1}, X^k) + \mathcal{D}_\phi(\tilde{X}^{k+1}, X^{k+1}) \\ &\leq \mathcal{D}_\phi(P, X^k) - \mathcal{D}_\phi(P, X^{k+1}) - \mathcal{D}_\phi(\tilde{X}^{k+1}, X^k) + \mu_k, \end{aligned} \quad (3.7)$$

where the second equality follows from the three points identity in Lemma 1. Moreover, since  $\tilde{X}^{k+1} \in \Omega$  and  $P \in \Omega$ , then  $\langle \Delta^k, \tilde{X}^{k+1} - P \rangle \leq \|\tilde{X}^{k+1} - P\|_F \|\Delta^k\|_F \leq 2\rho\eta_k$ . Combining this with (3.6) and (3.7), we have

$$\langle C, \tilde{X}^{k+1} \rangle \leq \langle C, P \rangle + \varepsilon_k (\mathcal{D}_\phi(P, X^k) - \mathcal{D}_\phi(P, X^{k+1}) - \mathcal{D}_\phi(\tilde{X}^{k+1}, X^k)) + \varepsilon_k \mu_k + 2\rho\eta_k + \nu_k, \quad \forall P \in \Omega. \quad (3.8)$$

Now, set  $P = \tilde{X}^k$  in (3.8), we see that

$$\begin{aligned} \langle C, \tilde{X}^{k+1} \rangle &\leq \langle C, \tilde{X}^k \rangle + \varepsilon_k (\mathcal{D}_\phi(\tilde{X}^k, X^k) - \mathcal{D}_\phi(\tilde{X}^k, X^{k+1}) - \mathcal{D}_\phi(\tilde{X}^{k+1}, X^k)) + \varepsilon_k \mu_k + 2\rho\eta_k + \nu_k \\ &\leq \langle C, \tilde{X}^k \rangle - \varepsilon_k (\mathcal{D}_\phi(\tilde{X}^k, X^{k+1}) + \mathcal{D}_\phi(\tilde{X}^{k+1}, X^k)) + \varepsilon_k (\mu_{k-1} + \mu_k) + 2\rho\eta_k + \nu_k \\ &\leq \langle C, \tilde{X}^k \rangle + \varepsilon_k (\mu_{k-1} + \mu_k) + 2\rho\eta_k + \nu_k. \end{aligned} \quad (3.9)$$

Note that  $\{\langle C, \tilde{X}^k \rangle\}$  is bounded below since  $\tilde{X}^k$  is in the compact set  $\Omega$  for all  $k$ . Then, since  $0 < \underline{\varepsilon} \leq \varepsilon_k \leq \bar{\varepsilon} < \infty$ ,  $\sum \nu_k < \infty$ ,  $\sum \eta_k < \infty$  and  $\sum \mu_k < \infty$ , it follows from (3.9) and Lemma 2 that  $\{\langle C, \tilde{X}^k \rangle\}$  is convergent. Also, we see from (3.9) that

$$\varepsilon_k (\mathcal{D}_\phi(\tilde{X}^k, X^{k+1}) + \mathcal{D}_\phi(\tilde{X}^{k+1}, X^k)) \leq \langle C, \tilde{X}^k \rangle - \langle C, \tilde{X}^{k+1} \rangle + \varepsilon_k (\mu_{k-1} + \mu_k) + 2\rho\eta_k + \nu_k.$$

From this, together with  $0 < \varepsilon \leq \varepsilon_k \leq \bar{\varepsilon} < \infty$ ,  $\nu_k \rightarrow 0$ ,  $\eta_k \rightarrow 0$ ,  $\mu_k \rightarrow 0$  and the fact that  $\{\langle C, \tilde{X}^k \rangle\}$  is convergent, we get that

$$\mathcal{D}_\phi(\tilde{X}^k, X^{k+1}) \rightarrow 0 \quad \text{and} \quad \mathcal{D}_\phi(\tilde{X}^{k+1}, X^k) \rightarrow 0.$$

Next, let  $X^*$  be an arbitrary optimal solution of (3.1) (hence (1.1)). Obviously,  $\langle C, X^* \rangle \leq \langle C, \tilde{X}^{k+1} \rangle$  for all  $k$  since  $\tilde{X}^{k+1} \in \Omega$ . By setting  $P = X^*$  in (3.8), we see that

$$\begin{aligned} 0 &\leq \mathcal{D}_\phi(X^*, X^{k+1}) \\ &\leq \mathcal{D}_\phi(X^*, X^k) + \varepsilon_k^{-1}(\langle C, X^* \rangle - \langle C, \tilde{X}^{k+1} \rangle) - \mathcal{D}_\phi(\tilde{X}^{k+1}, X^k) + \mu_k + \varepsilon_k^{-1}(2\rho\eta_k + \nu_k) \\ &\leq \mathcal{D}_\phi(X^*, X^k) + \mu_k + \varepsilon_k^{-1}(2\rho\eta_k + \nu_k). \end{aligned} \quad (3.10)$$

Thus, we can conclude from the above inequality and Lemma 2 that  $\{\mathcal{D}_\phi(X^*, X^k)\}$  is convergent. On the other hand, since  $\{\tilde{X}^k\}$  is bounded (due to  $\tilde{X}^k \in \Omega$ ), it has at least one cluster point. Suppose that  $\tilde{X}^\infty$  is a cluster point and  $\{\tilde{X}^{k_i}\}$  is a convergent subsequence such that  $\lim_{i \rightarrow \infty} \tilde{X}^{k_i} = \tilde{X}^\infty$ . Then, by using (3.8) with  $P = X^*$  again, we have for all  $k_i$ ,

$$\begin{aligned} \langle C, \tilde{X}^{k_i} \rangle &\leq \langle C, X^* \rangle + \varepsilon_{k_i-1}(\mathcal{D}_\phi(X^*, X^{k_i-1}) - \mathcal{D}_\phi(X^*, X^{k_i}) - \mathcal{D}_\phi(\tilde{X}^{k_i}, X^{k_i-1})) \\ &\quad + \varepsilon_{k_i-1}\mu_{k_i-1} + 2\rho\eta_{k_i-1} + \nu_{k_i-1} \\ &\leq \langle C, X^* \rangle + \varepsilon_{k_i-1}(\mathcal{D}_\phi(X^*, X^{k_i-1}) - \mathcal{D}_\phi(X^*, X^{k_i})) + \varepsilon_{k_i-1}\mu_{k_i-1} + 2\rho\eta_{k_i-1} + \nu_{k_i-1}. \end{aligned}$$

Then, passing to the limit and recalling that  $\{\mathcal{D}_\phi(X^*, X^k)\}$  is convergent,  $0 < \varepsilon \leq \varepsilon_k \leq \bar{\varepsilon} < \infty$ ,  $\nu_k \rightarrow 0$ ,  $\eta_k \rightarrow 0$ ,  $\mu_k \rightarrow 0$ , we obtain that

$$\langle C, \tilde{X}^\infty \rangle \leq \langle C, X^* \rangle.$$

Note that  $\tilde{X}^\infty \in \Omega$  since  $\Omega$  is closed. Thus,  $\tilde{X}^\infty$  is an optimal solution of (3.1) (hence (1.1)).

In addition, from Property 1(i) and the fact that  $\{\mathcal{D}_\phi(X^*, X^k)\}$  is convergent, we can conclude that  $\{X^k\}$  must be bounded and hence it has at least one cluster point. Suppose that  $X^\infty$  is a cluster point and  $\{X^{k_j}\}$  is a convergent subsequence such that  $\lim_{j \rightarrow \infty} X^{k_j} = X^\infty$ . Then, from  $\mathcal{D}_\phi(\tilde{X}^{k_j}, X^{k_j}) \leq \mu_{k_j-1} \rightarrow 0$ , the boundedness of  $\{\tilde{X}^{k_j}\}$  and Property 1(iii), we have that  $\lim_{j \rightarrow \infty} \tilde{X}^{k_j} = X^\infty$ . Therefore, from what we have proved in the last paragraph,  $X^\infty$  is an optimal solution of (3.1) (hence (1.1)), and moreover, by using (3.10) with  $X^*$  replaced by  $X^\infty$ , we can conclude that  $\{\mathcal{D}_\phi(X^\infty, X^k)\}$  is convergent. On the other hand, it follows from  $\lim_{j \rightarrow \infty} X^{k_j} = X^\infty$  and Property 1(ii) that  $\mathcal{D}_\phi(X^\infty, X^{k_j}) \rightarrow 0$ . Consequently,  $\{\mathcal{D}_\phi(X^\infty, X^k)\}$  must converge to zero. Now, let  $\hat{X}^\infty$  be any cluster point of  $\{X^k\}$  with a subsequence  $\{X^{k'_j}\}$  such that  $X^{k'_j} \rightarrow \hat{X}^\infty$ . Since  $\mathcal{D}_\phi(X^\infty, X^k) \rightarrow 0$ , we have  $\mathcal{D}_\phi(X^\infty, X^{k'_j}) \rightarrow 0$ . Using Property 1(iii) again, we see that  $X^\infty = \hat{X}^\infty$ . Since  $\hat{X}^\infty$  is arbitrary, we can conclude that  $\lim_{k \rightarrow \infty} X^k = X^\infty$ . This, together with the boundedness of  $\{\tilde{X}^k\}$ ,  $\mathcal{D}_\phi(\tilde{X}^k, X^k) \rightarrow 0$  and Property 1(iii), implies that  $\{\tilde{X}^k\}$  also converges to  $X^\infty$ . We then complete the proof.  $\square$

From Theorem 1, we see that the convergence of our iEPPA can be easily guaranteed with proper choices of  $\{\varepsilon_k\}$ ,  $\{\nu_k\}$ ,  $\{\eta_k\}$  and  $\{\mu_k\}$ . To make our iEPPA truly implementable, we should also address how to efficiently solve the subproblem (3.2) to find a pair  $(X^k, \tilde{X}^k)$  satisfying condition (3.3) at each iteration (see **Step 1** in Algorithm 1). Note that the subproblem (3.2) has the same form as the entropic regularized counterpart of problem (1.1). Then, one can follow [6] to apply the Dykstra's algorithm with Kullback-Leibler projections (DyKL) for solving it. In this paper, we shall adapt an alternative method presented in the next section to solve (3.2). Our numerical experiments show that our method is more efficient than DyKL for solving (3.2) with a fixed  $\varepsilon_k$  and hence can be of independent interest for solving an entropic regularized problem in form of (3.2).

## 4 A dual block coordinate descent method for solving (3.2)

In this section, we present an alternative method for solving the subproblem (3.2). Specifically, we first derive the dual problem of (3.2), which is conceivably more tractable, and then apply a block coordinate

descent (BCD) method for solving it. For notational simplicity, we drop the index  $k$  and consider the following generic problem with given  $S \in \mathbb{R}_{++}^{n_1 \times n_2 \times n_3}$  and  $\varepsilon > 0$ :

$$\begin{aligned} \min_{X \in \mathbb{R}^{n_1 \times n_2 \times n_3}} \quad & \langle C, X \rangle + \varepsilon \mathcal{D}_\phi(X, S) \\ \text{s.t.} \quad & \mathcal{A}^{(i)}(X) - \mathbf{b}^{(i)} = 0, \quad i = 1, \dots, N, \\ & X \leq U, \end{aligned} \quad (4.1)$$

where  $\phi(X) = \sum_{rst} X_{rst} \log X_{rst} - X_{rst}$ . By introducing an auxiliary variable  $Z \in \mathbb{R}^{n_1 \times n_2 \times n_3}$  and substituting  $\phi$  into (4.1), we can further reformulate problem (4.1) as

$$\begin{aligned} \min_{X, Z \in \mathbb{R}^{n_1 \times n_2 \times n_3}} \quad & \langle M, X \rangle + \varepsilon \sum_{r,s,t} X_{rst} (\log X_{rst} - 1) + \delta_+(Z) \\ \text{s.t.} \quad & \mathcal{A}^{(i)}(X) - \mathbf{b}^{(i)} = 0, \quad i = 1, \dots, N, \\ & X + Z = U, \end{aligned} \quad (4.2)$$

where  $M := C - \varepsilon \log S$  and  $\delta_+(\cdot)$  is the indicator function over the set  $\{Z \in \mathbb{R}^{n_1 \times n_2 \times n_3} : Z \geq 0\}$ . The Lagrangian function associated with (4.2) is

$$\begin{aligned} \mathcal{L}(X, Z, \mathbf{y}^{(1)}, \dots, \mathbf{y}^{(N)}, W) = & \langle M - \sum_{i=1}^N \mathcal{A}^{(i,*)} \mathbf{y}^{(i)} - W, X \rangle + \varepsilon \sum_{r,s,t} X_{rst} (\log X_{rst} - 1) \\ & + \delta_+(Z) - \langle W, Z \rangle + \sum_{i=1}^N \langle \mathbf{y}^{(i)}, \mathbf{b}^{(i)} \rangle + \langle W, U \rangle, \end{aligned}$$

where  $\mathbf{y}^{(i)} \in \mathbb{R}^{m_i}$  ( $1 \leq i \leq N$ ),  $W \in \mathbb{R}^{n_1 \times n_2 \times n_3}$  are Lagrangian multipliers for (4.2) and  $\mathcal{A}^{(i,*)} : \mathbb{R}^{m_i} \rightarrow \mathbb{R}^{n_1 \times n_2 \times n_3}$  is the adjoint mapping of  $\mathcal{A}^{(i)}$  that is defined by  $\mathcal{A}^{(i,*)} \mathbf{y}^{(i)} := \sum_{j=1}^{m_i} y_j^{(i)} A_j^{(i)}$ . Then, the dual problem of (4.2) is given by

$$\max_{\mathbf{y}^{(1)}, \dots, \mathbf{y}^{(N)}, W} \left\{ \min_{X, Z} \mathcal{L}(X, Z, \mathbf{y}^{(1)}, \dots, \mathbf{y}^{(N)}, W) \right\}. \quad (4.3)$$

Observe that

$$\min_X \left\{ \left\langle M - \sum_{i=1}^N \mathcal{A}^{(i,*)} \mathbf{y}^{(i)} - W, X \right\rangle + \varepsilon \sum_{r,s,t} X_{rst} (\log X_{rst} - 1) \right\} = -\varepsilon \left\langle \widetilde{M}, \exp \left( \varepsilon^{-1} (W + \sum_{i=1}^N \mathcal{A}^{(i,*)} \mathbf{y}^{(i)}) \right) \right\rangle,$$

where  $\widetilde{M} := \exp(-M/\varepsilon) = S \circ \exp(-C/\varepsilon)$  and

$$\min_Z \{ \delta_+(Z) - \langle W, Z \rangle \} = \begin{cases} 0, & \text{if } W \leq 0, \\ -\infty, & \text{otherwise.} \end{cases}$$

Here the notation  $\exp(X)$  means that the exponential operation is applied to all entries of  $X$ . With these facts and some manipulations, problem (4.3) is then equivalent to

$$\min_{\mathbf{y}^{(1)}, \dots, \mathbf{y}^{(N)}, W} \left\{ R(\mathbf{y}^{(1)}, \dots, \mathbf{y}^{(N)}, W) \right. \\ \left. := \varepsilon \left\langle \widetilde{M}, \exp \left( \varepsilon^{-1} (W + \sum_{i=1}^N \mathcal{A}^{(i,*)} \mathbf{y}^{(i)}) \right) \right\rangle - \sum_{i=1}^N \langle \mathbf{y}^{(i)}, \mathbf{b}^{(i)} \rangle - \langle W, U \rangle + \delta_-(W) \right\}, \quad (4.4)$$

where  $\delta_-(\cdot)$  is the indicator function over the set  $\{W \in \mathbb{R}^{n_1 \times n_2 \times n_3} : W \leq 0\}$ . Now, we see that problem (4.4) is a convex problem with  $N + 1$  separable blocks of variables and thus is conceivably more tractable than the original problem (4.1). Indeed, for this kind of problems containing several separable blocks of variables, it is desirable to apply the BCD method, which basically minimizes the objective  $R$  with respect to  $\mathbf{y}^{(1)}, \dots, \mathbf{y}^{(N)}, W$  cyclically at each iteration. The iterative scheme of the dual BCD method for solving (4.1) is presented as Algorithm 2.

We will show in the next subsection that the dual BCD in Algorithm 2 is R-linearly convergent and also provides an optimal solution of problem (4.1). Moreover, by using the nice structures imposed on  $\mathcal{A}^{(i)}$  ( $i = 1, \dots, N$ ) in Assumption 1 together with some careful manipulations as presented in subsection

---

**Algorithm 2** A dual block coordinate descent method for solving (4.1)

---

**Input:** Choose  $(\mathbf{y}^{(1),0}, \dots, \mathbf{y}^{(N),0}, W^0) \in \text{dom } R$  arbitrarily. Set  $\ell = 0$ .

**while** a termination criterion is not met, **do**

**Step 1.** compute

$$\begin{aligned} \mathbf{y}^{(i),\ell+1} &= \arg \min_{\mathbf{y}^{(i)}} R(\mathbf{y}^{(1),\ell+1}, \dots, \mathbf{y}^{(i-1),\ell+1}, \mathbf{y}^{(i)}, \mathbf{y}^{(i+1),\ell}, \dots, \mathbf{y}^{(N),\ell}, W^\ell), \quad 1 \leq i \leq N, \\ W^{\ell+1} &= \arg \min_W R(\mathbf{y}^{(1),\ell+1}, \dots, \mathbf{y}^{(N),\ell+1}, W). \end{aligned} \quad (4.5)$$

**Step 2.** Set  $\ell = \ell + 1$  and go to **Step 1**.

**end while**

**Output:**  $(\mathbf{y}^{(1),\ell}, \dots, \mathbf{y}^{(N),\ell}, W^\ell)$

---

4.3, one can show that all subproblems in our dual BCD method admit closed-form solutions which leads to the following explicit iterative scheme:

$$\begin{aligned} \mathbf{y}^{(i),\ell+1} &= \varepsilon \log \mathbf{b}^{(i)} - \varepsilon \log \left( \mathcal{A}^{(i)} \left( \widetilde{M} \circ \exp \left( \varepsilon^{-1} \sum_{q=1}^{i-1} \mathcal{A}^{(q,*)} \mathbf{y}^{(q),\ell+1} \right. \right. \right. \\ &\quad \left. \left. \left. + \varepsilon^{-1} \sum_{q=i+1}^N \mathcal{A}^{(q,*)} \mathbf{y}^{(q),\ell} \right) \circ \exp \left( \varepsilon^{-1} W^\ell \right) \right), \quad 1 \leq i \leq N, \\ W^{\ell+1} &= \min \left\{ \varepsilon \log \left( U ./ \left( \widetilde{M} \circ \exp \left( \sum_{q=1}^N \mathcal{A}^{(q,*)} \mathbf{y}^{(q),\ell+1} \right) \right), 0 \right\}. \end{aligned} \quad (4.6)$$

Alternatively, for any  $\ell \geq 0$ , let  $\boldsymbol{\xi}^{(i),\ell} := \exp(\varepsilon^{-1} \mathbf{y}^{(i),\ell})$  for  $1 \leq i \leq N$  and  $\Gamma^\ell := \exp(\varepsilon^{-1} W^\ell)$ , then the iterative scheme (4.6) can be equivalently written as

$$\begin{aligned} \boldsymbol{\xi}^{(i),\ell+1} &= \mathbf{b}^{(i)} ./ \mathcal{A}^{(i)} \left( \widetilde{M} \circ (\mathcal{A}^{(1,\bullet)} \boldsymbol{\xi}^{(1),\ell+1}) \circ \dots \circ (\mathcal{A}^{(i-1,\bullet)} \boldsymbol{\xi}^{(i-1),\ell+1}) \right. \\ &\quad \left. \circ (\mathcal{A}^{(i+1,\bullet)} \boldsymbol{\xi}^{(i+1),\ell}) \circ \dots \circ (\mathcal{A}^{(N,\bullet)} \boldsymbol{\xi}^{(N),\ell}) \circ \Gamma^\ell \right), \quad 1 \leq i \leq N, \\ \Gamma^{\ell+1} &= \min \left\{ U ./ \left( \widetilde{M} \circ (\mathcal{A}^{(1,\bullet)} \boldsymbol{\xi}^{(1),\ell+1}) \circ \dots \circ (\mathcal{A}^{(N,\bullet)} \boldsymbol{\xi}^{(N),\ell+1}) \right), 1 \right\}. \end{aligned} \quad (4.7)$$

Here, for any  $\mathbf{z} \in \mathbb{R}^{m_i}$ , the tensor  $\mathcal{A}^{(i,\bullet)} \mathbf{z} \in \mathbb{R}^{n_1 \times n_2 \times n_3}$  is defined as follows:

$$(\mathcal{A}^{(i,\bullet)} \mathbf{z})_{rst} = \begin{cases} (\mathcal{A}^{(i,*)} \mathbf{z})_{rst}, & \text{if } (r, s, t) \in \mathcal{J}^{(i)}, \\ 1, & \text{otherwise,} \end{cases}$$

where  $\mathcal{J}^{(i)}$  is the aggregated non-zero pattern of  $\mathcal{A}^{(i,*)}$  defined by

$$\mathcal{J}^{(i)} = \{ (r, s, t) \mid (A_j^{(i)})_{rst} \neq 0 \text{ for some } j \in \{1, \dots, m_i\} \}. \quad (4.8)$$

**Remark 1.** For the efficient implementation of (4.7), it is more convenient to introduce the following tensors for  $1 \leq i \leq N$ :

$$\begin{aligned} \widehat{M}^{(i),\ell+1} &= \widetilde{M} \circ (\mathcal{A}^{(1,\bullet)} \boldsymbol{\xi}^{(1),\ell+1}) \circ \dots \circ (\mathcal{A}^{(i-1,\bullet)} \boldsymbol{\xi}^{(i-1),\ell+1}) \circ (\mathcal{A}^{(i+1,\bullet)} \boldsymbol{\xi}^{(i+1),\ell}) \circ \dots \circ (\mathcal{A}^{(N,\bullet)} \boldsymbol{\xi}^{(N),\ell}) \circ \Gamma^\ell, \\ \widehat{M}^{(N+1),\ell+1} &= \widetilde{M} \circ (\mathcal{A}^{(1,\bullet)} \boldsymbol{\xi}^{(1),\ell+1}) \circ \dots \circ (\mathcal{A}^{(N,\bullet)} \boldsymbol{\xi}^{(N),\ell+1}). \end{aligned}$$

Then, the  $\ell$ -th cycle of the BCD scheme in (4.7) can be carried out as follows.

$$\begin{aligned} \widehat{M}^{(1),\ell+1} &= \left( \widehat{M}^{(N+1),\ell} ./ (\mathcal{A}^{(1,\bullet)} \boldsymbol{\xi}^{(1),\ell}) \right) \circ \Gamma^\ell, & \boldsymbol{\xi}^{(1),\ell+1} &= \mathbf{b}^{(1)} ./ \mathcal{A}^{(1)} \left( \widehat{M}^{(1),\ell+1} \right), \\ \widehat{M}^{(i),\ell+1} &= \left( \widehat{M}^{(i-1),\ell+1} ./ (\mathcal{A}^{(i,\bullet)} \boldsymbol{\xi}^{(i),\ell}) \right) \circ (\mathcal{A}^{(i-1,\bullet)} \boldsymbol{\xi}^{(i-1),\ell+1}), & \boldsymbol{\xi}^{(i),\ell+1} &= \mathbf{b}^{(i)} ./ \mathcal{A}^{(i)} \left( \widehat{M}^{(i),\ell+1} \right), \quad 2 \leq i \leq N, \\ \widehat{M}^{(N+1),\ell+1} &= \left( \widehat{M}^{(N),\ell+1} ./ \Gamma^\ell \right) \circ (\mathcal{A}^{(N,\bullet)} \boldsymbol{\xi}^{(N),\ell+1}), & \Gamma^{\ell+1} &= \min \left\{ U ./ \widehat{M}^{(N+1),\ell+1}, 1 \right\}. \end{aligned}$$

Note that in the actual implementation of (4.7), only a single tensor is used to store  $\widehat{M}^{(i),\ell+1}$  for  $i = 1, \dots, N+1$ , and it is repeatedly overwritten and updated.

Note that both iterative schemes (4.6) and (4.7) are simple and easy-to-implement. The main computational complexity for (4.7) is  $\mathcal{O}(n_1 n_2 n_3)$ . In particular, since the iterative scheme (4.7) only needs elementwise multiplications and the simple  $\min(\cdot)$  operation, it can be much more efficient than (4.6) in practice. However, like the Sinkhorn's algorithm, (4.7) may also suffer from numerical instabilities when  $\varepsilon$  takes a small value. Hence, in the unlikely event where  $\varepsilon$  is a small value in our iEPPA, one can use (4.6) instead to carry on all computations in the log domain and perform the *log-sum-exp* (see, e.g., [28, Section 4.4]) technique for avoiding underflow/overflow. Fortunately, as we mentioned in Section 3, the proximal parameter  $\varepsilon_k$  involved in our iEPPA does not need to take a very small value to obtain an accurate solution of the original problem (3.1) (hence (1.1)). This is also evident from our experiments which indicate that  $\varepsilon = 0.05$  is sufficient for obtaining fairly accurate solutions. Therefore, we can safely use the efficient iterative scheme (4.7) as a subroutine in our iEPPA.

In addition, we are aware that there is a close connection between the Dykstra's algorithm with Bregman projection (including DyKL as a special case) and (block) coordinate descent methods, although to the best of our knowledge, such a connection has not been stated explicitly until the recent work by Tibshirani [36]. Indeed, one can deduce from [36, Section 5] that the DyKL algorithm used in [6] for solving the entropic regularized problem in form of (4.1) (see Appendix B for the DyKL algorithm applied to the case of the 2-marginal capacity constrained optimal transport problem) is equivalent to the BCD method applied to a certain dual problem given by

$$\min_{\Lambda_i \in \mathbb{R}^{n_1 \times n_2 \times n_3}, i=1, \dots, N+1} \Phi^* \left( \nabla \Phi(K) - \sum_{i=1}^{N+1} \Lambda_i \right) + \sum_{i=1}^{N+1} \delta_{\mathcal{S}_i}^*(\Lambda_i), \quad (4.9)$$

where  $\Phi(X) := \sum_{rst} X_{rst} \log X_{rst}$ ,  $K := S \circ \exp(-C/\varepsilon)$ ,  $\mathcal{S}_i := \{X : \mathcal{A}^{(i)}(X) = b^{(i)}\}$  for  $i = 1, \dots, N$ ,  $\mathcal{S}_{N+1} := \{X : X \leq U\}$ , and  $\delta_{\mathcal{S}_i}^*$  is the conjugate of the indicator function  $\delta_{\mathcal{S}_i}$ . It is clear that the dual problem (4.9) is different from ours in (4.4). Therefore, the DyKL algorithm and our dual BCD method are not equivalent to each other. Moreover, our dual BCD method (either (4.6) or (4.7)) consumes much less memory. Because our dual variables  $(\mathbf{y}^{(1)}, \dots, \mathbf{y}^{(N)}, W)$  only need  $\sum_{i=1}^N m_i + n_1 n_2 n_3$  units of memory, while the dual variables  $(\Lambda_1, \dots, \Lambda_{N+1})$  in (4.9) need  $(N+1)n_1 n_2 n_3$  units of memory.

## 4.1 Convergence results for dual BCD

We next show the convergence results for our dual BCD method in Algorithm 2. It is worth noting that the (block) coordinate descent method enjoys a long history for solving the problem (containing (4.4) as a special case) of minimizing a class of convex differentiable functions over a certain closed convex set; see, for example, [25, 26, 37]. Hence, our main convergence results are simply derived by revisiting these classic works.

We first show the existence of optimal solutions of problems (4.1) and (4.4), and their relations in the following proposition whose proof can be found in Appendix A.1.

**Proposition 1.** *Suppose that Assumption 2 holds. Then, the optimal solutions of problems (4.1) and (4.4) exist. Moreover, for any optimal solution  $(\bar{\mathbf{y}}^{(1)}, \dots, \bar{\mathbf{y}}^{(N)}, \bar{W})$  of problem (4.4),*

$$\bar{X} := \exp \left( \varepsilon^{-1} \left( \sum_{i=1}^N \mathcal{A}^{(i,*)} \bar{\mathbf{y}}^{(i)} + \bar{W} - M \right) \right) \quad (4.10)$$

*is an optimal solution of problem (4.1).*

Next we present the main convergence results for our dual BCD method based on the theory developed in [25]. To make the paper self-contained, we provide its proof in Appendix A.2.

**Theorem 2 (Convergence of dual BCD).** *Let  $\{(\mathbf{y}^{(1),\ell}, \dots, \mathbf{y}^{(N),\ell}, W^\ell)\}$  be the sequence generated by the dual BCD method in Algorithm 2, and let*

$$X^\ell := \exp \left( \varepsilon^{-1} \left( \sum_{i=1}^N \mathcal{A}^{(i,*)} \mathbf{y}^{(i),\ell} + W^\ell - M \right) \right).$$

*Then, the following statements hold.*

- (i)  $\{(\mathbf{y}^{(1),\ell}, \dots, \mathbf{y}^{(N),\ell}, W^\ell)\}$  converges  $R$ -linearly to an optimal solution of problem (4.4).
- (ii)  $\{X^\ell\}$  converges  $R$ -linearly to an optimal solution of problem (4.1).

## 4.2 Implementable verification of condition (3.3)

From the previous subsection, we know that the dual BCD method can be safely applied for solving the subproblem (3.2) in our iEPPA. In this subsection, we shall discuss how to verify condition (3.3) at a point returned by our dual BCD method.

We first assume that there is a procedure  $\mathcal{G}$  such that for any  $0 \leq X \leq U$ , after performing the procedure  $\mathcal{G}$  on  $X$ , we can obtain that  $\mathcal{G}(X) \in \Omega$  and  $\|\mathcal{G}(X) - X\|_F \leq c \sum_{i=1}^N \|\mathbf{r}^{(i)}\|$  for some constant  $c > 0$ , where  $\mathbf{r}^{(i)} := \mathbf{b}^{(i)} - \mathcal{A}^{(i)}(X)$  ( $i = 1, \dots, N$ ) are residuals. Since  $\Omega$  is a polyhedron, such a procedure is typically achievable in practice. We give three examples as follows.

- If the projection of a point  $X$  onto  $\Omega$  (denoted by  $P_\Omega(X)$ ) is easy to compute, one can directly use  $\mathcal{G} = P_\Omega$ . In this case, from the Hoffman error bound theorem [18], there exists a constant  $c > 0$  such that  $\|\mathcal{G}(X) - X\|_F \leq c \sum_{i=1}^N \|\mathbf{r}^{(i)}\|$ .
- For the standard 2-marginal OT problem, where  $\Omega = \{X \in \mathbb{R}^{m \times n} : X\mathbf{1}_n = \mathbf{a}, X^\top \mathbf{1}_m = \mathbf{b}, X \geq 0\}$ , one can consider the efficient rounding procedure used in [2, Algorithm 2] as  $\mathcal{G}$ .
- Suppose that a relative interior point  $X^{\text{ri}}$  of  $\Omega$  is available on hand, i.e.,  $\mathcal{A}^{(i)}(X^{\text{ri}}) = \mathbf{b}^{(i)}$ ,  $i = 1, \dots, N$ , and  $0 < X^{\text{ri}} < U$ . Note that such a point can be obtained for many choices of  $\mathcal{A}^{(i)}$  and  $U$ . For example, in the 2-marginal COT problem,  $\Omega$  is formed by  $\{X \in \mathbb{R}^{m \times n} : X\mathbf{1}_n = \mathbf{a}, X^\top \mathbf{1}_m = \mathbf{b}, 0 \leq X \leq U\}$ . If  $U > \mathbf{a}\mathbf{b}^\top$ , then  $\mathbf{a}\mathbf{b}^\top$  is obviously a relative interior point. Otherwise, one can apply a certain alternating projection method to find a point in the intersection of  $\{X \in \mathbb{R}^{m \times n} : X\mathbf{1}_n = \mathbf{a}\}$ ,  $\{X \in \mathbb{R}^{m \times n} : X^\top \mathbf{1}_m = \mathbf{b}\}$  and  $\{X \in \mathbb{R}^{m \times n} : \epsilon \leq X \leq U - \epsilon\}$  with some small  $\epsilon > 0$ . Having an available relative interior point  $X^{\text{ri}}$  on hand, we can then perform the following procedure. We first compute the projection of  $X$  onto  $\bar{\Omega} := \{X \in \mathbb{R}^{m \times n} : \mathcal{A}^{(i)}(X) = \mathbf{b}^{(i)}, i = 1, \dots, N\}$ , which is in general easier than  $P_\Omega$ . Let  $Z := P_{\bar{\Omega}}(X)$  and  $V' := Z - X$ . It follows from the Hoffman error bound theorem that  $\|V'\|_F \leq c' \sum_{i=1}^N \|\mathbf{r}^{(i)}\|$  with some  $c' > 0$ . Then, if  $0 \leq Z \leq U$ , we are done. Otherwise, we consider a point  $\tilde{X} = Z + \lambda(X^{\text{ri}} - Z)$  with  $0 \leq \lambda \leq 1$ . It is easy to see that  $\mathcal{A}^{(i)}(\tilde{X}) = \mathbf{b}^{(i)}$  for  $i = 1, \dots, N$ . By choosing

$$\lambda = \max \left\{ \max_{(r,s,t) \in \mathcal{J}_1} \left\{ \frac{Z_{rst} - U_{rst}}{Z_{rst} - X_{rst}^{\text{ri}}} \right\}, \max_{(r,s,t) \in \mathcal{J}_2} \left\{ \frac{-Z_{rst}}{X_{rst}^{\text{ri}} - Z_{rst}} \right\} \right\},$$

where  $\mathcal{J}_1 := \{(r, s, t) : Z_{rst} > U_{rst}\}$  and  $\mathcal{J}_2 := \{(r, s, t) : Z_{rst} < 0\}$ , we can also ensure that  $0 \leq \tilde{X} \leq U$  and hence  $\tilde{X} \in \Omega$ . Moreover, note from  $Z = X + V'$  and  $0 \leq X \leq U$  that

$$\begin{aligned} \lambda &= \max \left\{ \max_{(r,s,t) \in \mathcal{J}_1} \left\{ \frac{X_{rst} + V'_{rst} - U_{rst}}{Z_{rst} - X_{rst}^{\text{ri}}} \right\}, \max_{(r,s,t) \in \mathcal{J}_2} \left\{ \frac{-X_{rst} - V'_{rst}}{X_{rst}^{\text{ri}} - Z_{rst}} \right\} \right\} \\ &\leq \max \left\{ \max_{(r,s,t) \in \mathcal{J}_1} \left\{ \frac{V'_{rst}}{U_{rst} - X_{rst}^{\text{ri}}} \right\}, \max_{(r,s,t) \in \mathcal{J}_2} \left\{ \frac{-V'_{rst}}{X_{rst}^{\text{ri}}} \right\} \right\} \leq c'' \|V'\|_F, \end{aligned}$$

where  $c'' > 0$  is a constant depending only on  $U$  and  $X^{\text{ri}}$ . Then, we have

$$\begin{aligned} \|\tilde{X} - X\|_F &= \|Z + \lambda(X^{\text{ri}} - Z) - X\|_F \leq \lambda \|X^{\text{ri}} - Z\|_F + \|Z - X\|_F \\ &\leq \lambda (\|X^{\text{ri}} - X\|_F + \|Z - X\|_F) + \|Z - X\|_F \leq \lambda \|U\|_F + (1 + \lambda) \|V'\|_F \\ &\leq c'' \|U\|_F \|V'\|_F + 2 \|V'\|_F \leq (c'' \|U\|_F + 2) c' \sum_{i=1}^N \|\mathbf{r}^{(i)}\|. \end{aligned}$$

Therefore, the above procedure can be used as  $\mathcal{G}$ , i.e.,  $\mathcal{G}(X) = \tilde{X}$ .

Now, suppose that we have a dual point  $(\mathbf{y}^{(1),\ell+1}, \dots, \mathbf{y}^{(N),\ell+1}, W^{\ell+1})$  given by our dual BCD in Algorithm 2 at the  $\ell$ -th iteration, and compute a primal point by

$$X^{\ell+1} := \exp \left( \varepsilon^{-1} \left( \sum_{i=1}^N \mathcal{A}^{(i,*)} \mathbf{y}^{(i),\ell+1} + W^{\ell+1} - M \right) \right) \in \mathbb{R}_{++}^{n_1 \times n_2 \times n_3}.$$

From the optimality condition of the  $W$ -subproblem in (4.5) and  $\nabla \phi(X) = \log X$ , one can verify that

$$\begin{cases} 0 = C + \varepsilon(\log X^{\ell+1} - \log S) - W^{\ell+1} - \sum_{i=1}^N \mathcal{A}^{(i,*)} \mathbf{y}^{(i),\ell+1}, & (4.11a) \\ W^{\ell+1} \leq 0, \quad U - X^{\ell+1} \geq 0, \quad \langle W^{\ell+1}, U - X^{\ell+1} \rangle = 0, & (4.11b) \\ \mathbf{r}^{(i),\ell+1} = \mathbf{b}^{(i)} - \mathcal{A}^{(i)}(X^{\ell+1}), \quad 1 \leq i \leq N, & (4.11c) \end{cases}$$

where  $\mathbf{r}^{(1),\ell+1}, \dots, \mathbf{r}^{(N),\ell+1}$  are the residuals at the  $\ell$ -th iteration. Obviously, when  $\mathbf{r}^{(i),\ell+1} = 0$  for  $i = 1, \dots, N$ ,  $X^{\ell+1}$  is an exact optimal solution. However,  $\mathbf{r}^{(1),\ell+1}, \dots, \mathbf{r}^{(N),\ell+1}$  are generally nonzero vectors. We then perform the procedure  $\mathcal{G}$  on  $X^{\ell+1}$  to obtain that  $\tilde{X}^{\ell+1} = \mathcal{G}(X^{\ell+1}) \in \Omega \subseteq \Omega^\circ$  and  $\|V^{\ell+1}\|_F \leq c \sum_{i=1}^N \|\mathbf{r}^{(i),\ell+1}\|$  with  $V^{\ell+1} := \tilde{X}^{\ell+1} - X^{\ell+1}$ . Moreover, for any  $Y \in \Omega^\circ$ , we have

$$\begin{aligned} & \langle -W^{\ell+1} - \sum_{i=1}^N \mathcal{A}^{(i,*)} \mathbf{y}^{(i),\ell+1}, Y - \tilde{X}^{\ell+1} \rangle = -\langle W^{\ell+1}, Y - \tilde{X}^{\ell+1} \rangle \\ & = -\langle W^{\ell+1}, Y - U \rangle - \langle W^{\ell+1}, U - \tilde{X}^{\ell+1} \rangle \leq -\langle W^{\ell+1}, U - X^{\ell+1} - V^{\ell+1} \rangle \\ & = \langle W^{\ell+1}, V^{\ell+1} \rangle \leq \|W^{\ell+1}\|_F \|V^{\ell+1}\|_F \leq c \|W^{\ell+1}\|_F \sum_{i=1}^N \|\mathbf{r}^{(i),\ell+1}\| \leq c\tilde{c} \sum_{i=1}^N \|\mathbf{r}^{(i),\ell+1}\|, \end{aligned} \quad (4.12)$$

where the first equality follows because  $Y, \tilde{X}^{\ell+1} \in \Omega^\circ$  and hence  $\langle \sum_{i=1}^N \mathcal{A}^{(i,*)} \mathbf{y}^{(i),\ell+1}, Y - \tilde{X}^{\ell+1} \rangle = 0$ , the first inequality follows from  $W^{\ell+1} \leq 0$  and  $Y - U \leq 0$ , the third equality follows from (4.11b) and the last inequality follows because  $\{W^\ell\}$  is convergent (by Theorem 2(i)) and hence must be bounded from the above by some constant  $\tilde{c} > 0$ . Thus, for any  $\nu \geq 0$  such that  $c\tilde{c} \sum_{i=1}^N \|\mathbf{r}^{(i),\ell+1}\| \leq \nu$ , we can obtain from (4.12) that  $-W^{\ell+1} - \sum_{i=1}^N \mathcal{A}^{(i,*)} \mathbf{y}^{(i),\ell+1} \in \partial_\nu \delta_{\Omega^\circ}(\tilde{X}^{\ell+1})$ . This together with (4.11a) implies that

$$0 \in \partial_\nu \delta_{\Omega^\circ}(\tilde{X}^{\ell+1}) + C + \varepsilon(\nabla \phi(X^{\ell+1}) - \nabla \phi(S)).$$

From the above, we see that condition (3.3) can be verified at the candidate  $(X^{\ell+1}, \tilde{X}^{\ell+1})$  and can be satisfied when  $\sum_{i=1}^N \|\mathbf{r}^{(i),\ell+1}\|$  and  $\mathcal{D}_\phi(\tilde{X}^{\ell+1}, X^{\ell+1})$  are sufficiently small.

In view of the above, the verification of our inexact condition (3.3) is implementable. While for *either* Teboulle's inexact condition (3.4) *or* Eckstein's inexact condition (3.5), even though a feasible point  $\tilde{X}^{\ell+1} \in \Omega$  can be constructed successfully (for example, by the procedure  $\mathcal{G}$ ), one still cannot verify condition (3.4) *or* (3.5) at  $\tilde{X}^{\ell+1}$  because  $\tilde{X}^{\ell+1}$  may not lie in  $\mathbb{R}_{++}^{n_1 \times n_2 \times n_3}$  and hence  $\nabla \phi$  may not be defined at  $\tilde{X}^{\ell+1}$ . This shows the advantage of our inexact condition (3.3).

### 4.3 Computation of solutions of subproblems in dual BCD

In this subsection, we provide more details on the efficient computation of solutions of subproblems in the dual BCD method. Recall the iterative scheme in (4.5), for any  $1 \leq i \leq N$ ,  $\mathbf{y}^{(i),\ell+1}$  is computed by solving the following unconstrained minimization problem:

$$\min_{\mathbf{y}^{(i)}} \left\{ \varepsilon \left\langle \tilde{M}, \exp \left( \varepsilon^{-1} \left( \mathcal{A}^{(i,*)} \mathbf{y}^{(i)} + \sum_{q=1}^{i-1} \mathcal{A}^{(q,*)} \mathbf{y}^{(q),\ell+1} + \sum_{q=i+1}^N \mathcal{A}^{(q,*)} \mathbf{y}^{(q),\ell} + W^\ell \right) \right) \right\rangle \right. \\ \left. - \langle \mathbf{y}^{(i)}, \mathbf{b}^{(i)} \rangle \right\}. \quad (4.13)$$

Here we show how to solve (4.13) efficiently via the nice structures imposed on  $\mathcal{A}^{(i)}$  ( $i = 1, \dots, N$ ) in Assumption 1. To this end, we first give the following auxiliary proposition.

**Proposition 2.** *Suppose that Assumption 1 holds. Then, for any tensor  $M \in \mathbb{R}^{n_1 \times n_2 \times n_3}$  and any vector  $\mathbf{y}^{(i)} \in \mathbb{R}^{m_i}$ , we have*

$$\langle M, \exp(\varepsilon^{-1} \mathcal{A}^{(i,*)} \mathbf{y}^{(i)}) \rangle = \langle \mathcal{A}^{(i)}(M), \exp(\varepsilon^{-1} \mathbf{y}^{(i)}) \rangle + \sum_{(r,s,t) \notin \mathcal{J}^{(i)}} M_{rst},$$

where  $\mathcal{J}^{(i)}$  is defined in (4.8).

*Proof.* Note from Assumption 1 that  $A_j^{(i)}$  only has binary entries (0 or 1) for all  $j = 1, \dots, m_i$ , and the non-zero patterns of  $\{A_j^{(i)} \mid j = 1, \dots, m_i\}$  do not overlap with each other. Thus, one can see that

$$\begin{aligned} (\exp(\varepsilon^{-1} \mathcal{A}^{(i,*)} \mathbf{y}^{(i)}))_{rst} &= (\exp(\varepsilon^{-1} \sum_{j=1}^{m_i} A_j^{(i)} y_j^{(i)}))_{rst} \\ &= \begin{cases} \sum_{j=1}^{m_i} \exp(\varepsilon^{-1} y_j^{(i)}) (A_j^{(i)})_{rst}, & \text{if } (r, s, t) \in \mathcal{J}^{(i)}, \\ \exp(0) = 1, & \text{otherwise.} \end{cases} \end{aligned}$$

Let  $\kappa = \sum_{(r,s,t) \notin \mathcal{J}^{(i)}} M_{rst}$ . We then have that

$$\begin{aligned} \langle M, \exp(\varepsilon^{-1} \mathcal{A}^{(i,*)} \mathbf{y}^{(i)}) \rangle &= \kappa + \sum_{(r,s,t) \in \mathcal{J}^{(i)}} \sum_{j=1}^{m_i} \exp(\varepsilon^{-1} y_j^{(i)}) (A_j^{(i)})_{rst} M_{rst} \\ &= \kappa + \sum_{j=1}^{m_i} \exp(\varepsilon^{-1} y_j^{(i)}) \left( \sum_{(r,s,t) \in \mathcal{J}^{(i)}} (A_j^{(i)})_{rst} M_{rst} \right) = \kappa + \sum_{j=1}^{m_i} \exp(\varepsilon^{-1} y_j^{(i)}) \langle A_j^{(i)}, M \rangle \\ &= \kappa + \sum_{j=1}^{m_i} \exp(\varepsilon^{-1} y_j^{(i)}) (\mathcal{A}^{(i)}(M))_j. \end{aligned}$$

This completes the proof.  $\square$

Using Proposition 2, we can reformulate the first term in the objective function of (4.13) as below:

$$\begin{aligned} &\left\langle \widetilde{M}, \exp\left(\varepsilon^{-1} (\mathcal{A}^{(i,*)} \mathbf{y}^{(i)} + \sum_{q=1}^{i-1} \mathcal{A}^{(q,*)} \mathbf{y}^{(q),\ell+1} + \sum_{q=i+1}^N \mathcal{A}^{(q,*)} \mathbf{y}^{(q),\ell} + W^\ell)\right) \right\rangle \\ &= \left\langle \widetilde{M} \circ \exp\left(\varepsilon^{-1} (\sum_{q=1}^{i-1} \mathcal{A}^{(q,*)} \mathbf{y}^{(q),\ell+1} + \sum_{q=i+1}^N \mathcal{A}^{(q,*)} \mathbf{y}^{(q),\ell} + W^\ell)\right), \exp(\varepsilon^{-1} \mathcal{A}^{(i,*)} \mathbf{y}^{(i)}) \right\rangle \\ &= \left\langle \widetilde{M}^{(i),\ell} \circ \exp(\varepsilon^{-1} W^\ell), \exp(\varepsilon^{-1} \mathcal{A}^{(i,*)} \mathbf{y}^{(i)}) \right\rangle = \langle \mathcal{A}^{(i)}(\widetilde{M}^{(i),\ell} \circ \exp(\varepsilon^{-1} W^\ell)), \exp(\varepsilon^{-1} \mathbf{y}^{(i)}) \rangle + \Upsilon, \end{aligned}$$

where  $\widetilde{M}^{(i),\ell} := \widetilde{M} \circ \exp(\varepsilon^{-1} \sum_{q=1}^{i-1} \mathcal{A}^{(q,*)} \mathbf{y}^{(q),\ell+1} + \varepsilon^{-1} \sum_{q=i+1}^N \mathcal{A}^{(q,*)} \mathbf{y}^{(q),\ell})$  and  $\Upsilon$  is a constant independent of  $\mathbf{y}^{(i)}$ . Then,  $\mathbf{y}^{(i),\ell+1}$  can be simply computed by

$$\begin{aligned} \mathbf{y}^{(i),\ell+1} &= \arg \min_{\mathbf{y}^{(i)}} \left\{ \varepsilon \langle \mathcal{A}^{(i)}(\widetilde{M}^{(i),\ell} \circ \exp(\varepsilon^{-1} W^\ell)), \exp(\varepsilon^{-1} \mathbf{y}^{(i)}) \rangle - \langle \mathbf{y}^{(i)}, \mathbf{b}^{(i)} \rangle \right\} \\ &= \varepsilon \log \mathbf{b}^{(i)} - \varepsilon \log (\mathcal{A}^{(i)}(\widetilde{M}^{(i),\ell} \circ \exp(\varepsilon^{-1} W^\ell))). \end{aligned}$$

After obtaining  $\mathbf{y}^{(i),\ell+1}$ ,  $i = 1, \dots, N$ , we then update  $W^{\ell+1}$  by solving the following problem:

$$\begin{aligned} W^{\ell+1} &= \arg \min_W \left\{ \varepsilon \langle \widetilde{M}, \exp(\varepsilon^{-1} \sum_{q=1}^N \mathcal{A}^{(q,*)} \mathbf{y}^{(q),\ell+1} + \varepsilon^{-1} W) \rangle - \langle W, U \rangle + \delta_-(W) \right\}, \\ &= \min \{ \varepsilon \log (U / (\widetilde{M} \circ Y^{\ell+1})), 0 \}, \end{aligned}$$

where  $Y^{\ell+1} = \exp(\sum_{q=1}^N \mathcal{A}^{(q,*)} \mathbf{y}^{(q),\ell+1})$ .

## 5 Numerical experiments

In this section, we conduct numerical experiments to evaluate the performance of our iEPPA in Algorithm 1, which employs the dual BCD method in Algorithm 2 as a subroutine, for solving the 2-marginal and 3-marginal CMOT problems (1.3). More details on applying the dual BCD method for solving (4.1) with the constraints in (1.3) can be found in Appendix A.3. For the 2-marginal case, we compare our iEPPA with the Dykstra's algorithm with Kullback-Leibler projections (DyKL) adapted in [6] and the powerful commercial solver Gurobi (version 8.1.1 with an academic license). For ease of future reference, we briefly

recall the DyKL algorithm in Appendix B. For the 3-marginal case, we only compare our iEPPA with Gurobi. Moreover, we conduct experiments by applying our model (1.1) for solving simulated discrete tomography problems [38]. All experiments are run in MATLAB R2018b on a workstation with Intel Xeon processor E5-2680v3@2.50GHz (with 12 cores and 24 threads) and 128GB of RAM, equipped with 64-bit Windows 10 OS.

It is easy to show that the dual problem of (1.1) is

$$\max_{\mathbf{y}^{(1)}, \dots, \mathbf{y}^{(N)}, W} \left\{ \sum_{i=1}^N \langle \mathbf{b}^{(i)}, \mathbf{y}^{(i)} \rangle + \langle U, W \rangle : \sum_{i=1}^N \mathcal{A}^{(i,*)} \mathbf{y}^{(i)} + W \leq C, W \leq 0 \right\}, \quad (5.1)$$

and the Karush-Kuhn-Tucker (KKT) system for (1.1) and (5.1) is

$$\begin{aligned} \mathcal{A}^{(i)}(X) - \mathbf{b}^{(i)} &= 0, \quad i = 1, \dots, N, \quad \sum_{i=1}^N \mathcal{A}^{(i,*)} \mathbf{y}^{(i)} + W \leq C, \quad 0 \leq X \leq U, \\ \langle X, \sum_{i=1}^N \mathcal{A}^{(i,*)} \mathbf{y}^{(i)} + W - C \rangle &= 0, \quad \langle W, U - X \rangle = 0, \quad W \leq 0. \end{aligned} \quad (5.2)$$

where  $\mathbf{y}^{(1)}, \dots, \mathbf{y}^{(N)}$  and  $W$  are the Lagrangian multipliers (*or* dual variables). It is well known that when both the primal problem (1.1) and the dual problem (5.1) are feasible,  $(\widehat{X}, \widehat{\mathbf{y}}^{(1)}, \dots, \widehat{\mathbf{y}}^{(N)}, \widehat{W})$  satisfies the KKT system (5.2) if and only if  $\widehat{X}$  solves the primal problem (1.1) and  $(\widehat{\mathbf{y}}^{(1)}, \dots, \widehat{\mathbf{y}}^{(N)}, \widehat{W})$  solves the dual problem (5.1), respectively. Then, based on the KKT system (5.2), we define the relative KKT residual for any  $(X, \mathbf{y}^{(1)}, \dots, \mathbf{y}^{(N)}, W)$  as follows:

$$\Delta_{\text{kkt}} \left( := \Delta_{\text{kkt}}(X, \mathbf{y}^{(1)}, \dots, \mathbf{y}^{(N)}, W) \right) := \max \{ \Delta_i : 1 \leq i \leq 7 \},$$

where

$$\begin{aligned} \Delta_1(X) &:= \frac{(\sum_{i=1}^N \|\mathcal{A}^{(i)}(X) - \mathbf{b}^{(i)}\|^2)^{1/2}}{1 + (\sum_{i=1}^N \|\mathbf{b}^{(i)}\|^2)^{1/2}}, \\ \Delta_2(\mathbf{y}^{(1)}, \dots, \mathbf{y}^{(N)}, W) &:= \frac{\|\max \{ \sum_{i=1}^N \mathcal{A}^{(i,*)} \mathbf{y}^{(i)} + W - C, 0 \}\|_F}{1 + \|C\|_F}, \quad \Delta_3(X) := \frac{\|\min \{ X, 0 \}\|_F}{1 + \|X\|_F}, \\ \Delta_4(X) &:= \frac{\|\min \{ U - X, 0 \}\|_F}{1 + \|U\|_F}, \quad \Delta_5(W) := \frac{\|\max \{ W, 0 \}\|_F}{1 + \|W\|_F}, \quad \Delta_6(X, W) := \frac{|\langle W, U - X \rangle|}{1 + \|U\|_F}, \\ \Delta_7(X, \mathbf{y}^{(1)}, \dots, \mathbf{y}^{(N)}, W) &:= \frac{|\langle X, \sum_{i=1}^N \mathcal{A}^{(i,*)} \mathbf{y}^{(i)} + W - C \rangle|}{1 + \|C\|_F}. \end{aligned}$$

Obviously,  $(X, \mathbf{y}^{(1)}, \dots, \mathbf{y}^{(N)}, W)$  is a solution of the KKT system (5.2) if and only if  $\Delta_{\text{kkt}} = 0$ . We then use  $\Delta_{\text{kkt}}$  to set up the stopping criterion for iEPPA. Specifically, we terminate our iEPPA when

$$\Delta_{\text{kkt}}(X^{k+1}, \mathbf{y}^{(1),k+1}, \dots, \mathbf{y}^{(N),k+1}, W^{k+1}) < \text{Tol}_e,$$

where  $\text{Tol}_e$  is the tolerance which will be specified later, and  $X^{k+1}$  and  $(\mathbf{y}^{(1),k+1}, \dots, \mathbf{y}^{(N),k+1}, W^{k+1})$  are the approximate optimal solutions of the subproblem (3.2) and its corresponding dual problem, respectively, at the  $k$ -th iteration. The maximum number of iterations for iEPPA is set to be 500.

The performance of our iEPPA naturally depends on the efficiency of the dual BCD method in Algorithm 2 for solving the subproblem (3.2). Therefore, the choices of the proximal parameter  $\varepsilon$  and the stopping criterion for the subproblem at each iteration are vital for implementing the iEPPA. Note that a smaller regularization parameter  $\varepsilon$  would lead to a more difficult subproblem, and moreover, a very small  $\varepsilon$  may also cause numerical instabilities due to the loss of accuracy involving overflow/underflow operations. Fortunately, our iEPPA does not require  $\varepsilon$  to be very small in order to obtain a fairly accurate approximate solution of the original problem. In all our numerical experiments, we simply fix  $\varepsilon = 0.05$ . With this choice, we would not encounter any numerical instability and can safely use the iterative scheme (A.7) to solve the subproblem efficiently. On the other hand, as discussed in subsection 4.2, our inexact condition (3.3) is verifiable and can be satisfied as long as  $\sum_{i=1}^N \|\mathbf{r}^{(i),\ell+1}\|$  ( $\mathbf{r}^{(i),\ell+1} :=$

$\mathbf{b}^{(i)} - \mathcal{A}^{(i)}(X^{\ell+1})$ ,  $i = 1, \dots, N$ ) and  $\mathcal{D}_\phi(\tilde{X}^{\ell+1}, X^{\ell+1})$  are sufficiently small, where  $X^{\ell+1}$  is obtained by substituting  $(\mathbf{y}^{(1),\ell+1}, \dots, \mathbf{y}^{(N),\ell+1}, W^{\ell+1})$  into (4.10) at the  $\ell$ -th iteration and  $\tilde{X}^{\ell+1}$  can be constructed by  $\tilde{X}^{\ell+1} := \mathcal{G}(X^{\ell+1})$  with a proper procedure  $\mathcal{G}$ . Note that, with such a construction, we also have  $\|\tilde{X}^{\ell+1} - X^{\ell+1}\|_F \leq c \sum_{i=1}^N \|\mathbf{r}^{(i),\ell+1}\|$  for some constant  $c > 0$ . Hence, when  $\sum_{i=1}^N \|\mathbf{r}^{(i),\ell+1}\|$  is small, it is very likely that  $\mathcal{D}_\phi(\tilde{X}^{\ell+1}, X^{\ell+1})$  is small. In view of this, we would not explicitly construct  $\tilde{X}^{\ell+1}$  in our implementations to save computations, and terminate dual BCD when

$$\Delta_1(X^{\ell+1}) < \text{Tol}_{\text{sub}} := 0.99 \times \text{Tol}_e.$$

As observed from our experiments, this simple setting is sufficient to obtain a good performance. Of course, it is also possible to dynamically adjust  $\varepsilon$  and  $\text{Tol}_{\text{sub}}$  for further improving the numerical performance, but we will skip the investigation of such parameter tuning in this paper.

We also apply Gurobi 8.1.1 to solve problem (1.3). It is well known that Gurobi is a highly powerful and reliable solver for solving LPs. Therefore, we use the solution obtained by Gurobi as a benchmark to evaluate the quality of the solutions obtained by other methods. In our experiments, we use the default settings of Gurobi (allowing it to exploit multiple processors), but only choose the barrier method and disable the cross-over strategy. The reason is that as observed from our numerical tests, other methods (the primal/dual simplex method) embedded in Gurobi are in general not as efficient as the barrier method, and the cross-over strategy is usually too costly.

## 5.1 Experiments on synthetic data for 2-marginal CMOT

In this subsection, we consider the CMOT problem (1.3) in the 2-marginal case and generate simulated examples to test each algorithm. For each example, we first generate two discrete probability distributions denoted by

$$D_1 := \{(a_r, \mathbf{p}_r) \in \mathbb{R}_+ \times \mathbb{R}^3 : r = 1, \dots, n_1\} \quad \text{and} \quad D_2 := \{(b_s, \mathbf{q}_s) \in \mathbb{R}_+ \times \mathbb{R}^3 : s = 1, \dots, n_2\}.$$

Here,  $\mathbf{a} := (a_1, \dots, a_{n_1})^\top$  and  $\mathbf{b} := (b_1, \dots, b_{n_2})^\top$  are probabilities/weights generated from the standard uniform distribution on the open interval  $(0, 1)$ , and further normalized such that  $\sum_r^{n_1} a_r = \sum_s^{n_2} b_s = 1$ . Moreover,  $\{\mathbf{p}_r\}$  and  $\{\mathbf{q}_s\}$  are the support points whose entries are drawn from a Gaussian mixture distribution via the following MATLAB commands:

```
gm_num = 5; gm_mean = [-20; -10; 0; 10; 20];
sigma = zeros(1,1,gm_num); sigma(1,1,:) = 5*ones(gm_num,1);
gm_weights = rand(gm_num,1);
distrib = gmdistribution(gm_mean, sigma, gm_weights);
```

With these support points, the cost matrix  $C$  is generated by  $C_{rs} = \|\mathbf{p}_r - \mathbf{q}_s\|^2$  for  $1 \leq r \leq n_1$  and  $1 \leq s \leq n_2$  and normalized by dividing (element-wise) by its maximal entry.

We next describe how to generate an upper bound matrix  $U \in \mathbb{R}_{++}^{n_1 \times n_2}$ . Note that if most of the entries of  $U$  are too large (e.g.,  $U$  is a matrix of all ones), then such an upper bound matrix can be redundant. Conversely, if most of the entries of  $U$  are too small, then the feasible set of (1.3) can be empty and Assumption 2 fails to hold. Hence, a randomly generated upper bound matrix  $U$  is usually unsatisfactory for our testing purpose. Thanks to the special structure of the constraints in (1.3), one can easily see that  $P := \mathbf{a}\mathbf{b}^\top$  must lie in the set  $\{X \in \mathbb{R}^{n_1 \times n_2} : X\mathbf{1}_{n_2} = \mathbf{a}, X^\top\mathbf{1}_{n_1} = \mathbf{b}, X \geq 0\}$ . We then set  $U := 2P = 2\mathbf{a}\mathbf{b}^\top$  as the upper bound matrix. With this setting, Assumption 2 can be satisfied and our numerical results also indicate that such an upper bound matrix is generally not redundant.

### 5.1.1 Comparisons between Gurobi, iEPPA and DyKL

In this part of experiments, we evaluate the performances of Gurobi, iEPPA and DyKL. For DyKL, the entropic regularization parameter  $\varepsilon$  is chosen from  $\{10^{-1}, 10^{-2}, 10^{-3}, 10^{-4}\}$  in our numerical tests. For  $\varepsilon \in \{10^{-1}, 10^{-2}\}$ , we follow [6, Section 5.2] to implement DyKL directly, while for  $\varepsilon \in \{10^{-3}, 10^{-4}\}$ , we

adapt the *log-sum-exp* trick (see, for example, [28, Section 4.4]) to stabilize DyKL (see Appendix B for the implementations of DyKL). We terminate DyKL when  $\Delta_1(X^{k+1}) < \text{Tol}_d$ , where  $X^{k+1}$  is generated by DyKL at the  $k$ -th iteration. We also set  $\text{Tol}_e = \text{Tol}_d = 10^{-5}$ . Moreover, the maximum number of iterations for DyKL is set to be 20000.

Table 1 presents the computational results for different choices of  $(n_1, n_2)$ . In this table, “normalized obj” denotes the normalized objective function value defined as  $|\mathcal{F}^k - \mathcal{F}_g|/|\mathcal{F}_g|$ , where  $\mathcal{F}_g$  denotes the objective value returned by Gurobi and  $\mathcal{F}^k$  is the approximate objective function value obtained by each algorithm; “feasibility” denotes the primal feasibility accuracy, namely,  $\max\{\Delta_1, \Delta_3\}$ ; “time” denotes the total computational time (in seconds) and “iter” denotes the number of iterations. For Gurobi, we do not report its number of iterations and use “—” instead. For our iEPPA, we also record the total number of dual BCD iterations. For instance, the item “35(315)” means that iEPPA took 35 outer iterations and used a total of 315 dual BCD iterations.

Table 1: Numerical results on synthetic data for 2-marginal CMOT. In the table, “g” stands for Gurobi; “e” stands for iEPPA; “d1”, “d2”, “d3”, “d4” stand for DyKL with  $\varepsilon = 10^{-1}, 10^{-2}, 10^{-3}, 10^{-4}$ , respectively.

$n_1$	$n_2$	g	e	d1	d2	d3	d4	g	e	d1	d2	d3	d4
		normalized obj						feasibility					
4000	2000	0	6.08e-05	1.15e-01	2.77e-03	6.73e-04	7.54e-04	4.04e-08	9.83e-06	9.42e-06	9.88e-06	9.97e-06	1.00e-05
4000	4000	0	3.55e-05	1.77e-01	4.27e-03	2.09e-02	2.11e-02	1.24e-06	6.84e-06	8.75e-06	9.93e-06	9.95e-06	1.00e-05
4000	8000	0	8.14e-05	1.40e-01	4.87e-03	2.68e-03	2.76e-03	2.07e-06	4.68e-06	9.90e-06	9.77e-06	9.99e-06	1.00e-05
5000	2500	0	5.29e-05	1.44e-01	2.41e-03	4.73e-03	4.80e-03	7.97e-07	9.28e-06	7.37e-06	9.76e-06	9.96e-06	1.00e-05
5000	5000	0	5.27e-05	1.56e-01	3.97e-03	1.56e-03	1.69e-03	1.45e-06	5.47e-06	7.09e-06	9.62e-06	9.99e-06	9.99e-06
5000	10000	0	6.91e-05	1.92e-01	4.14e-03	6.72e-03	6.77e-03	2.42e-06	4.38e-06	7.88e-06	9.93e-06	9.97e-06	1.00e-05
6000	3000	0	9.63e-06	1.80e-01	3.53e-03	8.56e-03	8.61e-03	1.27e-06	6.71e-06	8.83e-06	9.81e-06	9.99e-06	1.00e-05
6000	6000	0	2.38e-05	1.05e-01	2.55e-03	7.36e-03	7.26e-03	2.63e-06	5.56e-06	9.74e-06	9.96e-06	9.99e-06	1.00e-05
6000	12000	0	4.55e-05	1.62e-01	3.32e-03	5.38e-03	5.52e-03	3.19e-06	3.37e-06	8.22e-06	9.92e-06	9.98e-06	1.00e-05
7000	3500	0	3.44e-05	1.25e-01	3.65e-03	2.58e-03	2.60e-03	1.68e-06	5.41e-06	6.83e-06	9.69e-06	9.98e-06	1.00e-05
7000	7000	0	9.34e-05	2.34e-01	5.97e-03	1.22e-02	1.27e-02	2.26e-06	3.85e-06	9.72e-06	9.88e-06	9.98e-06	1.00e-05
7000	14000	0	8.35e-06	1.35e-01	1.96e-03	4.13e-03	4.16e-03	2.71e-06	2.99e-06	7.06e-06	9.96e-06	9.97e-06	1.00e-05
		iter						time (in seconds)					
4000	2000	—	35 ( 315)	11	153	991	9848	48.4	12.3	0.8	11.0	112.5	1112.7
4000	4000	—	41 ( 229)	11	155	588	5911	223.7	47.2	3.3	44.5	266.3	2670.1
4000	8000	—	42 ( 194)	10	135	857	8617	595.1	89.2	6.1	78.4	791.5	7909.4
5000	2500	—	33 ( 231)	13	162	951	9546	174.3	32.3	3.1	36.2	335.4	3349.9
5000	5000	—	42 ( 205)	11	134	957	9549	525.0	71.8	5.2	60.3	683.8	6798.3
5000	10000	—	41 ( 184)	10	128	737	7425	1011.5	130.9	9.7	119.4	1055.1	10604.3
6000	3000	—	43 ( 244)	11	176	783	7873	279.5	54.6	3.8	58.0	403.1	4044.9
6000	6000	—	35 ( 239)	13	233	891	9133	682.8	96.1	8.9	154.3	913.6	9318.5
6000	12000	—	46 ( 189)	10	129	780	7828	1415.3	203.6	14.0	174.4	1576.8	15702.3
7000	3500	—	42 ( 218)	9	133	823	8316	401.5	70.2	4.3	59.7	571.5	5770.9
7000	7000	—	45 ( 186)	8	107	543	5424	790.6	137.4	7.7	99.1	755.2	7522.6
7000	14000	—	53 ( 218)	13	177	1109	11146	2464.8	316.3	24.0	318.8	2998.4	29835.7

From Table 1, one can observe that our iEPPA performs better than DyKL in the sense that iEPPA always returns a better approximate objective function value (using Gurobi as the benchmark) with a comparable feasibility accuracy in much less CPU time. The accuracy for the normalized objective function value returned by iEPPA is always at the level of  $10^{-5}$  or even smaller, while the accuracy of DyKL is usually at the level of  $10^{-3}$ . In particular, decreasing the value of  $\varepsilon$  from  $10^{-2}$  to  $10^{-4}$  in DyKL does not improve the accuracy for the objective function value, but is more time-consuming (this phenomenon is detailed more in Remark 2). Therefore, DyKL may not be an efficient algorithm for computing a high accurate solution. We can also see that the feasibility accuracy returned by Gurobi is at around the same level as those of iEPPA and DyKL when the problem size is large, implying that the setting of  $\text{Tol}_e = 10^{-5}$  is sufficient for our iEPPA in this part of experiments. Moreover, for large-scale problems, Gurobi is also very time-consuming. As an example, for the case where  $(n_1, n_2) = (7000, 14000)$

in Table 1, a large-scale LP containing  $9.8 \times 10^7$  box-constrained variables and 21000 equality constraints was solved. In this case, we see that Gurobi is about 8 times slower than our iEPPA.

**Remark 2.** For DyKL, the accuracy of the solution in terms of the normalized objective function value is supposed to become better when the regularization parameter  $\varepsilon$  becomes smaller. However, we only observe such a phenomenon when  $\varepsilon$  is decreased from  $10^{-1}$  to  $10^{-2}$ . When  $\varepsilon \in \{10^{-2}, 10^{-3}, 10^{-4}\}$ , the accuracy remains almost the same. The reason is that DyKL actually suffers from very slow convergence speed when  $\varepsilon$  is small and hence the stopping tolerance  $\text{Tol}_d = 10^{-5}$  is not sufficient for DyKL to obtain a good approximate solution. Indeed, when we set  $\text{Tol}_d = 10^{-7}$  and test DyKL with  $\varepsilon = 10^{-3}$  on the case with  $(n_1, n_2) = (4000, 2000)$  (same as the first instance in Table 1), the returned normalized objective function value is  $2.6 \times 10^{-5}$ , which is much smaller than the accuracy ( $6.7 \times 10^{-4}$ ) reported in Table 1. However, the computational time also increases to 569s, which is about 5 times longer than the reported number of 112s.

### 5.1.2 Comparisons between Gurobi and iEPPA

To further evaluate the performance of our iEPPA against Gurobi, we conduct more experiments on synthetic data with support points generated by the same Gaussian mixture distribution as in the previous set of experiments. In the following experiments, the number of rows  $n_1$  is fixed to be 1000, while the number of columns  $n_2$  varies from 1000 to 9000. The stopping tolerance  $\text{Tol}_\varepsilon$  for our iEPPA is set to be  $10^{-5}$ . The computational results are presented in Figure 1. From the results, we see that the “nobj” of iEPPA is always at the level of  $10^{-5}$ , which means that the objective function value returned by iEPPA is always close to that of Gurobi. Moreover, the feasibility accuracy of iEPPA remains at the level of  $10^{-6}$ , while the feasibility accuracy of Gurobi increases from the level of  $10^{-15}$  to  $10^{-6}$  as  $n_2$  increases. The computational time of either Gurobi or iEPPA increases almost linearly with respect to  $n_2$ , however, it is clear that the computational time taken by Gurobi grows much more rapidly than iEPPA. This is because when the problem size becomes large, the barrier method used in Gurobi may not be efficient enough and may also consume too much memory. In contrast, our iEPPA scales well with respect to the problem size and can be more favorable for solving the large-scale CMOT problem up to a moderate accuracy level of  $10^{-5}$ .

id	$n_1$	$n_2$	nobj		feas	
			g	e	g	e
1	1000	1000	0	4.4e-05	6.0e-15	9.8e-06
2	1000	2000	0	9.0e-05	4.8e-15	9.7e-06
3	1000	3000	0	7.3e-05	1.3e-07	9.7e-06
4	1000	4000	0	6.1e-05	4.7e-07	9.1e-06
5	1000	5000	0	1.9e-05	4.4e-07	6.8e-06
6	1000	6000	0	3.0e-05	7.5e-07	6.9e-06
7	1000	7000	0	3.2e-05	1.2e-06	6.2e-06
8	1000	8000	0	6.7e-05	1.2e-06	6.5e-06
9	1000	9000	0	9.2e-05	1.6e-06	5.2e-06

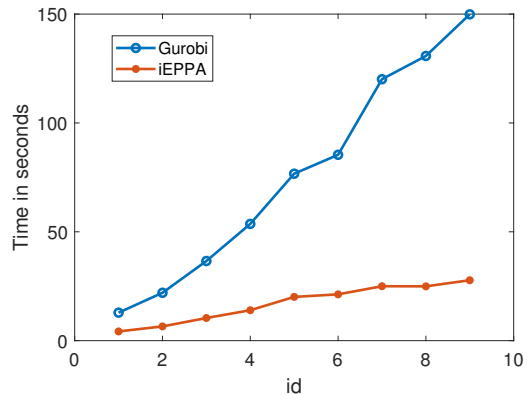


Figure 1: Comparisons between Gurobi and iEPPA for 2-marginal CMOT. In the table, “nobj” denotes the normalized objective function value, “feas” denotes the feasibility accuracy, “g” stands for Gurobi and “e” stands for iEPPA.

### 5.1.3 Comparisons between dual BCD and DyKL

We would like to point out that, besides the great efficiency of the iEPPA+BCD framework for solving the CMOT problem, applying our dual BCD method in Algorithm 2 for solving a *single* entropic regularized

CMOT problem (see (B.1)) is also possible. Here, we conduct an experiment to compare our dual BCD method and the DyKL for solving the entropic regularized CMOT problem with a fixed regularization parameter  $\varepsilon$ . We set  $\varepsilon = 10^{-3}$ ,  $n_1 = n_2 = 2000$  and terminate both methods when  $\Delta_1(X^{\ell+1}) < 10^{-7}$ , where  $X^{\ell+1}$  is generated by each method at the  $\ell$ -th iteration. The semilogy diagrams of the primal feasibility accuracy and the normalized objective function value (using Gurobi as the benchmark) with respect to the computational time are presented in Figure 2. From the figure, one can see that both dual BCD method and the DyKL are able to achieve the desired feasibility accuracy and attain almost the same normalized objective function value. However, the computational time of the dual BCD method and the DyKL in this test is 102s and 265s, respectively, that is, the dual BCD method is about 2.5 times faster than the DyKL in terms of the computational time. Indeed, by roughly calculating the number of flops, we see that, at each iteration, the dual BCD method needs  $(7n_1n_2 + n_1 + n_2)$  flops, while the DyKL needs  $(14n_1n_2 + n_1 + n_2)$  flops. Thus, based on the per-iteration complexity, the dual BCD method is about 2 times faster than the DyKL. Moreover, if the stabilization technique is applied for the DyKL (see (B.3)), the per-iteration complexity of the DyKL would become even worse. In view of the above, if one prefers to solve the entropic regularized problem with a fixed regularization parameter  $\varepsilon$ , our dual BCD method is still preferable over the Dykstra’s algorithm.

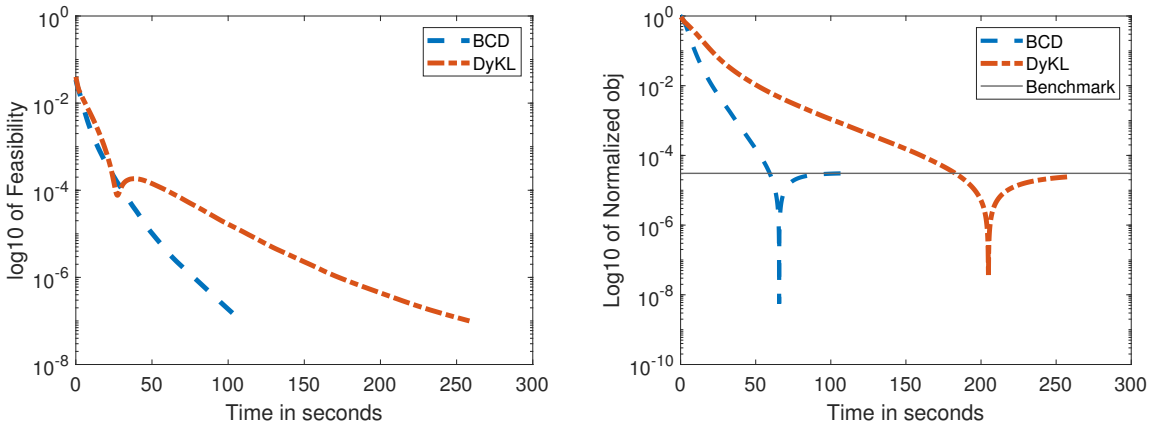


Figure 2: Comparisons between dual BCD and DyKL for solving the entropic regularized CMOT.

## 5.2 Experiments on synthetic data for 3-marginal CMOT

In this subsection, we consider the standard CMOT problem (1.3) in the 3-marginal case. Here, in view of the inferior performance of the DyKL presented in last section, we only generate synthetic instances to evaluate the performance of our iEPPA against Gurobi for saving space. Specially, we randomly generate three discrete probability distributions:  $D_1 = \{(a_r, \mathbf{p}_r) \in \mathbb{R}_+ \times \mathbb{R}^3 : r = 1, \dots, n_1\}$ ,  $D_2 = \{(b_s, \mathbf{q}_s) \in \mathbb{R}_+ \times \mathbb{R}^3 : s = 1, \dots, n_2\}$  and  $D_3 = \{(c_t, \mathbf{r}_t) \in \mathbb{R}_+ \times \mathbb{R}^3 : t = 1, \dots, n_3\}$ . Similar to the 2-marginal case in subsection 5.1, the marginals  $\mathbf{a} := (a_1, \dots, a_{n_1})^\top$ ,  $\mathbf{b} := (b_1, \dots, b_{n_2})^\top$  and  $\mathbf{c} := (c_1, \dots, c_{n_3})^\top$  are all generated independently from a uniformly distribution on the interval  $(0, 1)$ , respectively. Again, the marginals are normalized so that  $\sum_{r=1}^{n_1} a_r = \sum_{s=1}^{n_2} b_s = \sum_{t=1}^{n_3} c_t = 1$ . Moreover, the support points are generated independently from the same Gaussian mixture distribution given in subsection 5.1. Given these support points, we then compute the cost tensor  $C$  as follows:

$$C_{rst} := \|\mathbf{p}_r - \mathbf{q}_s\|^2 + \|\mathbf{q}_s - \mathbf{r}_t\|^2 + \|\mathbf{r}_t - \mathbf{p}_r\|^2, \quad \forall 1 \leq r \leq n_1, 1 \leq s \leq n_2, 1 \leq t \leq n_3.$$

We also normalize  $C$  by dividing it by its maximal entry. To generate a reasonable upper bound  $U$ , we adapt the same strategy as in the 2-marginal case to set  $U := 2(\mathbf{a} \otimes \mathbf{b} \otimes \mathbf{c})$ .

Figures 3–4 present comparisons between iEPPA and Gurobi. In this set of experiments, we always increase  $n_1$ , but fix  $n_2 = n_3$ , and set the stopping tolerance  $\text{Tol}_\varepsilon$  to be  $10^{-5}$ . We also plot the running time

to visualize the performance of each method. From the results, we can see that, similar to the 2-marginal case, our iEPPA is able to return moderately accurate approximate solutions and attain the desired primal feasibility accuracy. For large-scale problems, the feasibility accuracy of iEPPA is also comparable to that of Gurobi. For the computational time, *neither* Gurobi *nor* iEPPA increases approximately linearly with respect to  $n_1$ . However, our iEPPA is much faster than Gurobi for large-scale problems. Therefore, our iEPPA can be a more efficient method to obtain a solution with moderate accuracy for large-scale problems.

id	$n_1$	nobj		feas	
		g	e	g	e
1	400	0	5.0e-05	2.0e-12	9.8e-06
2	800	0	5.2e-05	2.5e-13	9.7e-06
3	1600	0	3.6e-05	4.1e-13	9.8e-06
4	3200	0	2.6e-05	2.2e-07	9.8e-06
5	6400	0	2.1e-05	9.4e-07	8.3e-06
6	128000	0	1.5e-05	1.8e-06	7.6e-06

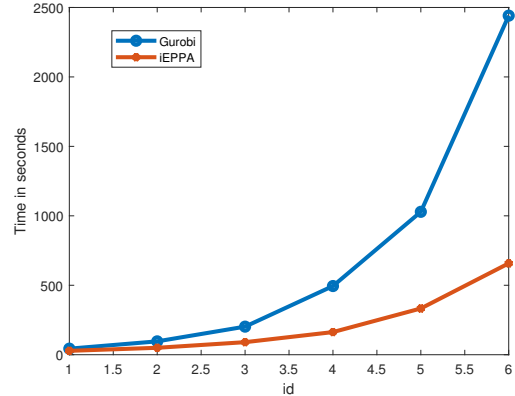


Figure 3: Comparisons between Gurobi and iEPPA for 3-marginal CMOT with  $n_2 = n_3 = 100$  and  $n_1 \in \{400, 800, 1600, 3200, 6400, 128000\}$ .

id	$n_1$	nobj		feas	
		g	e	g	e
1	4	0	3.5e-05	1.9e-11	9.7e-06
2	8	0	5.8e-05	2.8e-12	9.8e-06
3	16	0	3.1e-05	1.5e-12	9.8e-06
4	32	0	2.4e-05	1.9e-07	9.4e-06
5	64	0	1.3e-05	1.1e-07	7.5e-06
6	128	0	4.5e-06	1.7e-07	5.9e-06

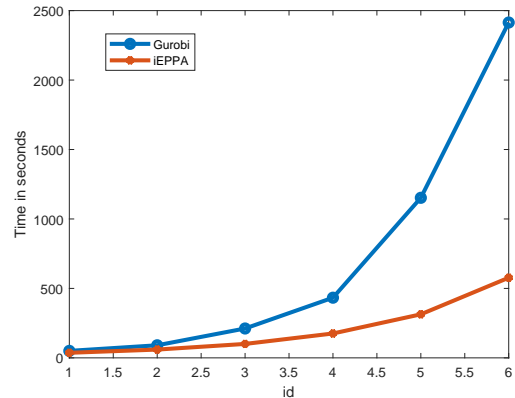


Figure 4: Comparisons between Gurobi and iEPPA for 3-marginal CMOT with  $n_2 = n_3 = 1000$  and  $n_1 \in \{4, 8, 16, 32, 64, 128\}$ .

### 5.3 Experiments on an application to discrete tomography

In this subsection, we conduct experiments on discrete tomography to illustrate the modeling capability of our model (1.1). We should mention that the purpose here is to present a preliminary investigation on the potential of using our model together with the iEPPA+BCD framework for solving the discrete tomography problem. A thorough numerical investigation is beyond the scope of this paper and will be left as a future research topic.

Let  $X$  be a 2D image of size  $n \times n$  and  $\vec{v}$  be a given direction that takes the form  $(1, p)$ ,  $(1, -p)$ ,  $(p, 1)$  or  $(p, -1)$  with  $p$  being a small nonnegative integer. In our experiments, a tomographic projection on the image  $X$  along  $\vec{v}$  is constructed as follows: we view the image  $X$  as a 2D grid of size  $n \times n$ , first pick all

lines which are parallel to the direction  $\vec{v}$  on this grid, then sum the entries on each line to form a vector. Such a projection then corresponds to a block of linear equality constraints of the form  $\mathbf{b}^{(i)} = \mathcal{A}^{(i)}(X)$  in our model. Figure 5 shows the constructions of the tomographic projection along directions  $(1, 0)$  and  $(2, 1)$ , respectively. The detailed construction can be found in Appendix C.

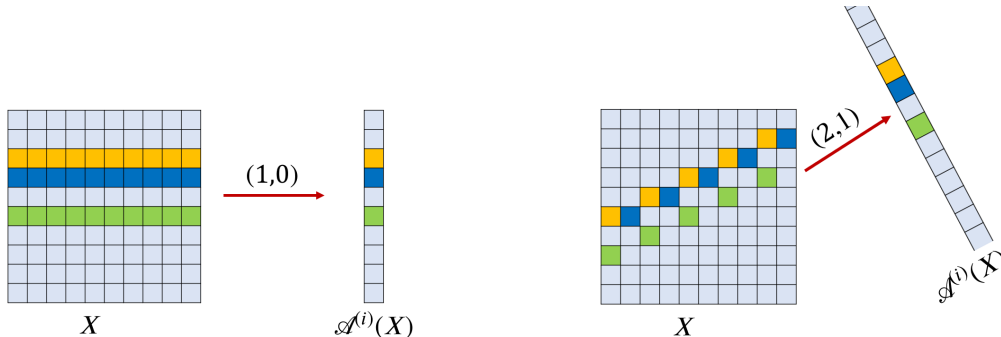


Figure 5: Examples of the operator  $\mathcal{A}^{(i)}$  for direction  $\vec{v} = (1, 0)$  (**left**) and direction  $\vec{v} = (2, 1)$  (**right**).

In Figure 6, we list five ground-truth images of size  $256 \times 256$  used in our experiments. For each of them, we compute  $N$  tomographic projections (which correspond to the linear mappings  $\mathcal{A}^{(i)}$ ,  $i = 1, \dots, N$  in our model) on this image along different directions to obtain  $\mathbf{b}^{(i)}$ ,  $i = 1, \dots, N$ . Then, our goal is to recover the original image from the collection of projections  $\{\mathbf{b}^{(i)}\}_{i=1}^N$  via applying our iEPPA+BCD framework for solving problem (1.1). Moreover, in our experiments, we set the entries of the cost matrix  $C \in \mathbb{R}^{n \times n}$  to be  $C_{rs} = |r - s|^2$  for  $1 \leq r, s \leq n$  and normalize  $C$  by dividing (element-wise) it by its maximal entry. We do not use any upper bound matrix  $U$  in the experiments. For our algorithm, we simply fix  $\varepsilon_k$  to be 0.05 and terminate our dual BCD at each iEPPA iteration when  $\Delta_1 < 10^{-4}$ .



Figure 6: Ground-truth images of size  $256 \times 256$  (from left to right): **flower**, **tree**, **animals**, **brain**, **chest**. Here, **flower**, **tree** and **animals** are artificial images, while **brain** and **chest** are taken from <https://radiopaedia.org/images/9219097> and <https://radiopaedia.org/cases/loculated-pneumothorax>, respectively.

Figure 7 presents the reconstructed images obtained by running 20 iEPPA iterations using different number of projections  $N$ . From the numerical results, we observe that our model (1.1) can faithfully recover all the images. Moreover, the quality of the recovered image is much better with more available projections. Thus, to improve the quality of the recovered image, a straightforward way is to increase the number of projections. Fortunately, for our approach of using model (1.1) and iEPPA+BCD, imposing more projections would not increase the computational cost dramatically since the main computational unit (which is one BCD iteration) only depends on  $N$  linearly. Specifically, for one more projection, we only need to add one more block of constraints in our model (1.1) and then correspondingly add one more block of dual variables in the dual BCD method.

**Remark 3.** To recover an  $n \times n$  image by our model (1.1) (which is an LP) with  $N$  available projections, the corresponding (sparse) coefficient matrix of the equality constraint has at least the size of  $Nn \times n^2$ . When  $n$  and  $N$  are large, such a large-scale problem can cause some LP solvers (e.g., Gurobi) to suffer from insufficient memory issues as well as high computational cost on an ordinary PC. We note that

another model (based on knowing a prior distribution) that aims to recover objects from a few tomographic projections is suggested in [1, 7]. In their framework, suppose that a 2D object with  $N$  projections is available. Then, the decision variable for the corresponding multi-marginal optimal transport problem will be a tensor of the order  $2 + N$  in the formulation given in [1]. Hence, it is difficult to implement the model efficiently. In addition, when the order of the tensor is large, the aforementioned model will invariably encounter memory issues. Moreover, our approach do not require any prior knowledge on the image to be recovered, which is another key feature that makes our modeling framework even more attractive.

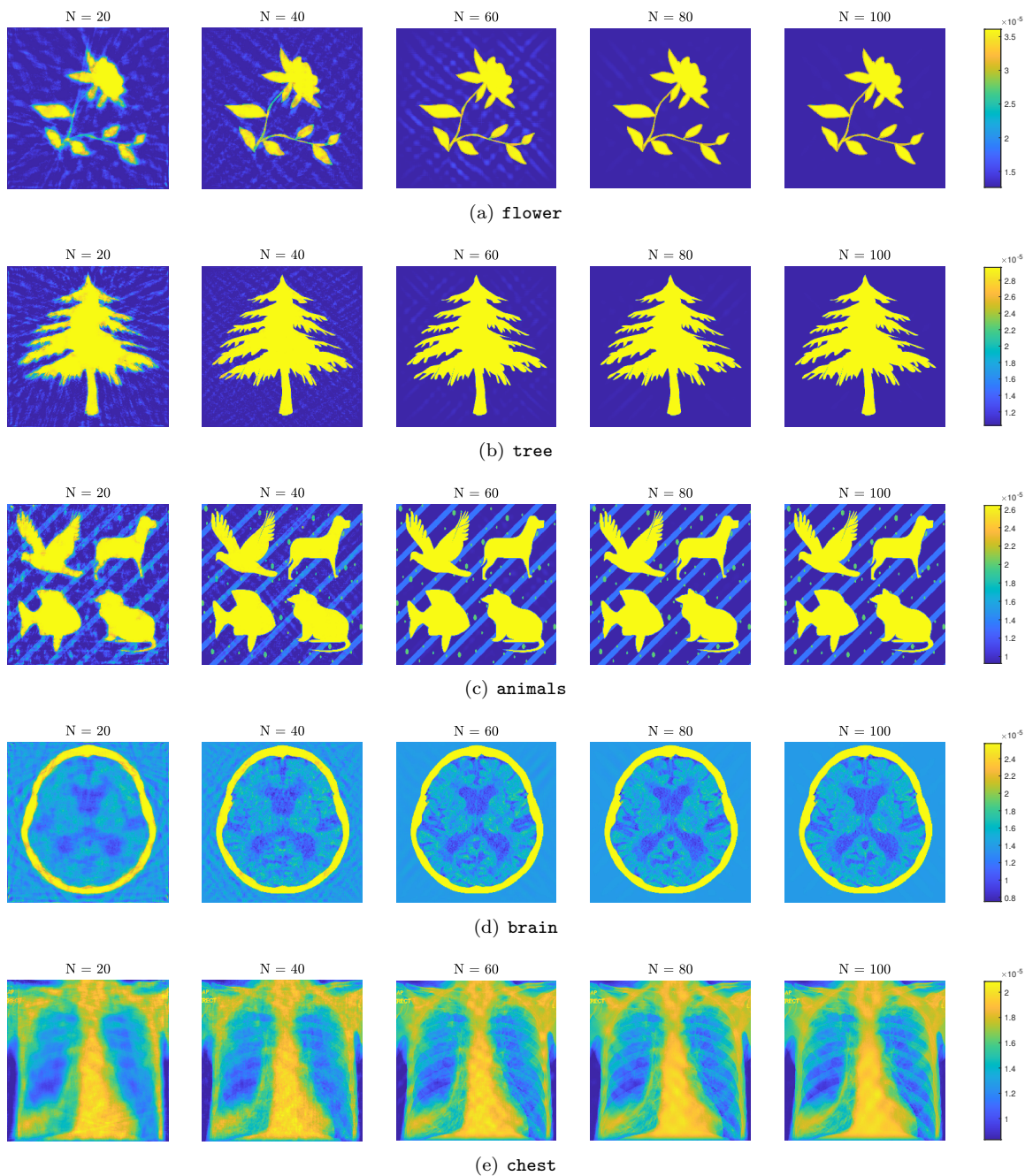


Figure 7: Reconstructed images using different number of projections  $N \in \{20, 40, 60, 80, 100\}$  by running 20 iEPPA iterations.

## 6 Concluding remarks

In this paper, we propose a class of linear programming (LP) problems that can be employed to efficiently model several application problems such as discrete tomography and disaggregation of input-output tables in economics. We then develop an implementable inexact entropic proximal point algorithm (iEPPA) for solving these specially structured LPs. To solve the subproblems that contain a special entropic proximal term, we adapt an easy-to-implement dual block coordinate descent (BCD) method to solve the associated more tractable dual subproblem. The convergence of our iEPPA and the R-linear convergence of the dual BCD method are also established. In particular, we develop a new practically verifiable inexact stopping condition for solving the iEPPA subproblem that has some computational advantages over those in the existing methods. Extensive numerical experiments have been conducted to demonstrate the high efficiency and robustness of our iEPPA+BCD framework for solving the capacity constrained multi-marginal optimal transport problem, in comparison to the Dykstra's algorithm with Kullback-Leibler projections and the commercial solver Gurobi. We also illustrate the potential modeling power of the proposed model by applying it to discrete tomography problems.

## Appendix A More details on the dual BCD method

### A.1 Proof of Proposition 1

First, problem (4.1) is equivalent to

$$\min_X \delta_{\Omega^\circ}(X) + \langle C, X \rangle + \varepsilon \mathcal{D}_\phi(X, S).$$

Since  $\text{dom } \phi = \mathbb{R}_+^{n_1 \times n_2 \times n_3}$  and thus  $\Omega^\circ \cap \text{dom } \phi = \Omega$  is nonempty (by Assumption 2) and bounded, then the objective function in the above problem is level bounded. Thus, a solution exists [31, Theorem 1.9] and must be unique since  $\phi$  is strictly convex. The essential smoothness of  $\phi$  further implies that the optimal solution can only lie in  $\mathbb{R}_{++}^{n_1 \times n_2 \times n_3}$ . Hence, the optimal solution of problem (4.2) also exists. Let  $(\bar{X}, \bar{Z}) \in \mathbb{R}_{++}^{n_1 \times n_2 \times n_3} \times \mathbb{R}_{++}^{n_1 \times n_2 \times n_3}$  be an optimal solution of problem (4.2). Since all constraint functions in (4.2) are affine and the set  $\{(X, Z) \in \mathbb{R}^{n_1 \times n_2 \times n_3} \times \mathbb{R}^{n_1 \times n_2 \times n_3} : Z \geq 0\}$  is a convex polyhedron, then it follows from [32, Theorem 3.25] that there exist multipliers  $\bar{\mathbf{y}}^{(i)} \in \mathbb{R}^{m_i}$ ,  $1 \leq i \leq N$  and  $\bar{W} \in \mathbb{R}^{n_1 \times n_2 \times n_3}$  such that

$$\begin{cases} 0 = M - \bar{W} - \sum_{i=1}^N \mathcal{A}^{(i,*)} \bar{\mathbf{y}}^{(i)} + \varepsilon \log \bar{X}, & \text{(A.1a)} \\ 0 \in -\bar{W} + \partial \delta_+(\bar{Z}), & \text{(A.1b)} \\ 0 = \mathbf{b}^{(i)} - \mathcal{A}^{(i)}(\bar{X}), \quad 1 \leq i \leq N, & \text{(A.1c)} \\ 0 = U - \bar{X} - \bar{Z}. & \text{(A.1d)} \end{cases}$$

Note from (A.1a) that

$$\bar{X} = \exp \left( \varepsilon^{-1} \left( \sum_{i=1}^N \mathcal{A}^{(i,*)} \bar{\mathbf{y}}^{(i)} + \bar{W} - M \right) \right).$$

Then, substituting this and (A.1d) into (A.1b) and (A.1c), recalling (1.4) and the fact that  $\partial \delta_+^* = \partial \delta_-$ , one can see that

$$\begin{cases} 0 = \mathbf{b}^{(i)} - \mathcal{A}^{(i)} \left( \exp \left( \varepsilon^{-1} \left( \sum_{i=1}^N \mathcal{A}^{(i,*)} \bar{\mathbf{y}}^{(i)} + \bar{W} - M \right) \right) \right), \quad i = 1, \dots, N, & \text{(A.2)} \\ 0 \in \exp \left( \varepsilon^{-1} \left( \sum_{i=1}^N \mathcal{A}^{(i,*)} \bar{\mathbf{y}}^{(i)} + \bar{W} - M \right) \right) - U + \partial \delta_-(\bar{W}). \end{cases}$$

This together with [32, Theorem 3.5] implies that  $(\bar{\mathbf{y}}^{(1)}, \dots, \bar{\mathbf{y}}^{(N)}, \bar{W})$  is an optimal solution of the dual problem (4.4) and hence the optimal solution of problem (4.4) exists.

Moreover, for any optimal solution  $(\hat{\mathbf{y}}^{(1)}, \dots, \hat{\mathbf{y}}^{(N)}, \widehat{W})$  of problem (4.4), it follows from [32, Theorem 3.5] that it satisfies the system (A.2) in place of  $(\bar{\mathbf{y}}^{(1)}, \dots, \bar{\mathbf{y}}^{(N)}, \bar{W})$ . Let

$$\widehat{X} := \exp \left( \varepsilon^{-1} \left( \sum_{i=1}^N \mathcal{A}^{(i,*)} \hat{\mathbf{y}}^{(i)} + \widehat{W} - M \right) \right), \quad \widehat{Z} := U - \widehat{X}.$$

Recall (1.4) and the fact that  $\partial\delta_- = \partial\delta_+$ , one can verify that  $(\widehat{X}, \widehat{Z}, \widehat{\mathbf{y}}^{(1)}, \dots, \widehat{\mathbf{y}}^{(N)}, \widehat{W})$  satisfies the system (A.1a)–(A.1d). Thus it follows from [32, Theorem 3.27] that  $(\widehat{X}, \widehat{Z})$  is an optimal solution of problem (4.2) and hence  $\widehat{X}$  is an optimal solution of problem (4.1). This completes the proof.

## A.2 Proof of Theorem 2

For the ease of applying the convergence results developed in [25], we first express problem (4.4) in the following compact form:

$$\min_{\boldsymbol{\chi}} \Psi(E\boldsymbol{\chi}) + \langle \mathbf{q}, \boldsymbol{\chi} \rangle \quad \text{s.t.} \quad \boldsymbol{\chi} \in \Xi, \quad (\text{A.3})$$

where  $\Psi : \mathbb{R}^{n_1 n_2 n_3} \rightarrow \mathbb{R}$  is defined by  $\Psi(\mathbf{y}) := \varepsilon \sum_i^{n_1 n_2 n_3} \exp((y_i - z_i)/\varepsilon)$ ,  $\mathbf{z} := \text{vec}(M) \in \mathbb{R}^{n_1 n_2 n_3}$ ,  $\mathbf{q} := -[\mathbf{b}^{(1)}; \dots; \mathbf{b}^{(N)}; \text{vec}(U)] \in \mathbb{R}^{\sum_{i=1}^N m_i + n_1 n_2 n_3}$ ,  $\boldsymbol{\chi} := [\mathbf{y}^{(1)}; \dots; \mathbf{y}^{(N)}; \text{vec}(W)] \in \mathbb{R}^{\sum_{i=1}^N m_i + n_1 n_2 n_3}$ ,  $\Xi := \{\boldsymbol{\chi} := [\mathbf{y}^{(1)}; \dots; \mathbf{y}^{(N)}; \text{vec}(W)] : W \leq 0\}$  and

$$E := [\text{vec}(A_1^{(1)}), \dots, \text{vec}(A_{m_1}^{(1)}), \dots, \text{vec}(A_1^{(N)}), \dots, \text{vec}(A_{m_N}^{(N)}), I_{n_1 n_2 n_3}] \in \mathbb{R}^{n_1 n_2 n_3 \times (\sum_{i=1}^N m_i + n_1 n_2 n_3)}.$$

One can easily verify that  $\text{dom } \Psi = \mathbb{R}^{n_1 n_2 n_3}$  is open and  $\Psi$  is strictly convex and twice continuously differentiable on  $\text{dom } \Psi$ .

Moreover, the optimal solution set of problem (A.3) is nonempty (by Proposition 1) and our dual BCD in Algorithm 2 indeed falls into the algorithmic framework in [25] for solving the problem in form of (A.3). Also, note from [25, Lemma 3.3] that the set  $\{E\boldsymbol{\chi} : \Psi(E\boldsymbol{\chi}) + \langle \mathbf{q}, \boldsymbol{\chi} \rangle \leq \alpha, \boldsymbol{\chi} \in \Xi\}$  is compact for any  $\alpha \in \mathbb{R}$ . Then, one can easily verify that  $\nabla^2 \Psi(E\boldsymbol{\chi}^*)$  is positive definite for any optimal solution  $\boldsymbol{\chi}^*$  of problem (A.3). Based on these facts, we can readily apply [25, Theorem 2.1] to obtain statement (i), i.e.,  $\boldsymbol{\chi}^t := (\mathbf{y}^{(1),t}, \dots, \mathbf{y}^{(N),t}, W^t) \rightarrow \boldsymbol{\chi}^*$  R-linearly.

We next prove statement (ii). Let  $\{(\widehat{\mathbf{y}}^{(1)}, \dots, \widehat{\mathbf{y}}^{(N)}, \widehat{W})\}$  be the limit of  $\{(\mathbf{y}^{(1),\ell}, \dots, \mathbf{y}^{(N),\ell}, W^\ell)\}$ . Then, one can see from statement (i) that  $\{(\widehat{\mathbf{y}}^{(1)}, \dots, \widehat{\mathbf{y}}^{(N)}, \widehat{W})\}$  is an optimal solution of problem (4.4) and further see from Proposition 1 that  $\widehat{X} := \exp((\sum_{i=1}^N \mathcal{A}^{(i,*)} \widehat{\mathbf{y}}^{(i)} + \widehat{W} - M)/\varepsilon)$  is an optimal solution of problem (4.1). Define the mapping  $\mathcal{H} : \mathbb{R}^{\sum_{i=1}^N m_i + n_1 n_2 n_3} \rightarrow \mathbb{R}^{n_1 n_2 n_3}$  by  $\mathcal{H}(\boldsymbol{\chi}) := \exp((E\boldsymbol{\chi} - \mathbf{m})/\varepsilon)$ , whose Jacobian matrix is given by  $J\mathcal{H}(\boldsymbol{\chi}) = \varepsilon^{-1} \text{Diag}[\exp((E\boldsymbol{\chi} - \mathbf{m})/\varepsilon)]E$ . Then, we see that  $\mathbf{x}^\ell := \text{vec}(X^\ell) = \mathcal{H}(\boldsymbol{\chi}^\ell)$  and  $\widehat{\mathbf{x}} := \text{vec}(\widehat{X}) = \mathcal{H}(\widehat{\boldsymbol{\chi}})$ , where  $\boldsymbol{\chi}^\ell := [\mathbf{y}^{(1),\ell}; \dots; \mathbf{y}^{(N),\ell}; \text{vec}(W^\ell)]$  and  $\widehat{\boldsymbol{\chi}} := [\widehat{\mathbf{y}}^{(1)}; \dots; \widehat{\mathbf{y}}^{(N)}; \text{vec}(\widehat{W})]$ . Moreover, we have

$$\begin{aligned} \|\mathbf{x}^\ell - \widehat{\mathbf{x}}\| &= \|\mathcal{H}(\boldsymbol{\chi}^\ell) - \mathcal{H}(\widehat{\boldsymbol{\chi}})\| = \left\| \left( \int_0^1 J\mathcal{H}(\widehat{\boldsymbol{\chi}} + \tau(\boldsymbol{\chi}^\ell - \widehat{\boldsymbol{\chi}})) d\tau \right) \cdot (\boldsymbol{\chi}^\ell - \widehat{\boldsymbol{\chi}}) \right\| \\ &\leq \left\| \int_0^1 J\mathcal{H}(\widehat{\boldsymbol{\chi}} + \tau(\boldsymbol{\chi}^\ell - \widehat{\boldsymbol{\chi}})) d\tau \right\| \cdot \|\boldsymbol{\chi}^\ell - \widehat{\boldsymbol{\chi}}\| \leq \int_0^1 \|J\mathcal{H}(\widehat{\boldsymbol{\chi}} + \tau(\boldsymbol{\chi}^\ell - \widehat{\boldsymbol{\chi}}))\| d\tau \cdot \|\boldsymbol{\chi}^\ell - \widehat{\boldsymbol{\chi}}\|, \end{aligned} \quad (\text{A.4})$$

where the second equality follows from the mean-value theorem. Note that

$$\Psi(E\widehat{\boldsymbol{\chi}}) + \langle \mathbf{q}, \widehat{\boldsymbol{\chi}} \rangle \leq \Psi(E\boldsymbol{\chi}^\ell) + \langle \mathbf{q}, \boldsymbol{\chi}^\ell \rangle \leq \Psi(E\boldsymbol{\chi}^0) + \langle \mathbf{q}, \boldsymbol{\chi}^0 \rangle, \quad \forall \ell \geq 0.$$

It then follows from [25, Lemma 3.3] that  $\{E\boldsymbol{\chi}^\ell\}$  is bounded. With this fact, one can easily verify that  $\|J\mathcal{H}(\widehat{\boldsymbol{\chi}} + \tau(\boldsymbol{\chi}^\ell - \widehat{\boldsymbol{\chi}}))\|$  is uniformly bounded from above by some constant  $L$ , i.e.,  $\|J\mathcal{H}(\widehat{\boldsymbol{\chi}} + \tau(\boldsymbol{\chi}^\ell - \widehat{\boldsymbol{\chi}}))\| \leq L$  for all  $\ell \geq 0$  and  $\tau \in [0, 1]$ . This together with (A.4) and statement (i) prove statement (ii).

## A.3 The dual BCD method for the CMOT problem (1.3)

As a special case of problem (1.1), the 3-marginal capacity constrained optimal transport problem (1.3) (which takes the linear mappings defined in (1.2)) has attracted particular attention. In this section, we write down the concrete iterative scheme of the dual BCD method in Algorithm 2 for solving (4.1) with the constraints in (1.3). We use  $\mathbf{f}, \mathbf{g}, \mathbf{h}, W$  to denote Lagrangian multipliers with respect to the following four constraints

$$\begin{aligned} \sum_{s,t} X_{rst} &= a_r, \quad r = 1, \dots, n_1, & \sum_{r,t} X_{rst} &= b_s, \quad s = 1, \dots, n_2, \\ \sum_{r,s} X_{rst} &= c_t, \quad t = 1, \dots, n_3, & X &\leq U, \end{aligned}$$

respectively. By using similar arguments as in Section 4, one obtains the dual subproblem:

$$\begin{aligned} \min_{\mathbf{f}, \mathbf{g}, \mathbf{h}, W} R(\mathbf{f}, \mathbf{g}, \mathbf{h}, W) &:= \varepsilon \sum_{r,s,t} \exp((f_r + g_s + h_t + W_{rst} - M_{rst})/\varepsilon) - \langle \mathbf{f}, \mathbf{a} \rangle \\ &\quad - \langle \mathbf{g}, \mathbf{b} \rangle - \langle \mathbf{h}, \mathbf{c} \rangle - \langle W, U \rangle + \delta_-(W), \end{aligned} \quad (\text{A.5})$$

where  $M := C - \varepsilon \log S$ . We then apply the BCD method for solving (A.5). Specifically, start from any  $(\mathbf{f}^0, \mathbf{g}^0, \mathbf{h}^0, W^0) \in \text{dom } R$ , at the  $\ell$ -th iteration, compute

$$\begin{aligned} \mathbf{f}^{\ell+1} &= \arg \min_{\mathbf{f}} R(\mathbf{f}, \mathbf{g}^\ell, \mathbf{h}^\ell, W^\ell), & \mathbf{g}^{\ell+1} &= \arg \min_{\mathbf{g}} R(\mathbf{f}^{\ell+1}, \mathbf{g}, \mathbf{h}^\ell, W^\ell), \\ \mathbf{h}^{\ell+1} &= \arg \min_{\mathbf{h}} R(\mathbf{f}^{\ell+1}, \mathbf{g}^{\ell+1}, \mathbf{h}, W^\ell), & W^{\ell+1} &= \arg \min_W R(\mathbf{f}^{\ell+1}, \mathbf{g}^{\ell+1}, \mathbf{h}^{\ell+1}, W). \end{aligned}$$

After some manipulations, one can obtain the following explicit iterative scheme:

$$\begin{aligned} \mathbf{f}^{\ell+1} &= \varepsilon \log(\mathbf{a}) - \varepsilon \log \left( \left[ \sum_{s,t} \exp((g_s^\ell + h_t^\ell + W_{rst}^\ell - M_{rst})/\varepsilon) \right]_{r=1}^{n_1} \right), \\ \mathbf{g}^{\ell+1} &= \varepsilon \log(\mathbf{b}) - \varepsilon \log \left( \left[ \sum_{r,t} \exp((f_r^{\ell+1} + h_t^\ell + W_{rst}^\ell - M_{rst})/\varepsilon) \right]_{s=1}^{n_2} \right), \\ \mathbf{h}^{\ell+1} &= \varepsilon \log(\mathbf{c}) - \varepsilon \log \left( \left[ \sum_{r,s} \exp((f_r^{\ell+1} + g_s^{\ell+1} + W_{rst}^\ell - M_{rst})/\varepsilon) \right]_{t=1}^{n_3} \right), \\ W^{\ell+1} &= \min \{ \varepsilon \log U + M - \mathbf{f}^{\ell+1} \otimes \mathbf{1}_{n_2} \otimes \mathbf{1}_{n_3} - \mathbf{1}_{n_1} \otimes \mathbf{g}^{\ell+1} \otimes \mathbf{1}_{n_3} - \mathbf{1}_{n_1} \otimes \mathbf{1}_{n_2} \otimes \mathbf{h}^{\ell+1}, 0 \}, \end{aligned} \quad (\text{A.6})$$

where  $\mathbf{1}_{n_i}$  denotes the  $n_i$ -dimensional vector of all ones for  $i = 1, 2, 3$ . Moreover, let  $\widetilde{M} := \exp(-M/\varepsilon)$ ,  $\tilde{\mathbf{f}}^\ell := \exp(\mathbf{f}^\ell/\varepsilon)$ ,  $\tilde{\mathbf{g}}^\ell := \exp(\mathbf{g}^\ell/\varepsilon)$ ,  $\tilde{\mathbf{h}}^\ell := \exp(\mathbf{h}^\ell/\varepsilon)$  and  $\widetilde{W}^\ell := \exp(W^\ell/\varepsilon)$ . Then, we can equivalently rewrite the iterative scheme (A.6) as

$$\begin{aligned} \tilde{\mathbf{f}}^{\ell+1} &= \mathbf{a} ./ \left( \left[ \sum_{s,t} (\widetilde{W}^\ell \circ \widetilde{M})_{rst} \tilde{g}_s^\ell \tilde{h}_t^\ell \right]_{r=1}^{n_1} \right), & \tilde{\mathbf{g}}^{\ell+1} &= \mathbf{b} ./ \left( \left[ \sum_{r,t} (\widetilde{W}^\ell \circ \widetilde{M})_{rst} \tilde{f}_r^{\ell+1} \tilde{h}_t^\ell \right]_{s=1}^{n_2} \right), \\ \tilde{\mathbf{h}}^{\ell+1} &= \mathbf{c} ./ \left( \left[ \sum_{r,s} (\widetilde{W}^\ell \circ \widetilde{M})_{rst} \tilde{f}_r^{\ell+1} \tilde{g}_s^{\ell+1} \right]_{t=1}^{n_3} \right), & \widetilde{W}^{\ell+1} &= \min \left\{ (U ./ \widetilde{M}) ./ (\tilde{\mathbf{f}}^{\ell+1} \otimes \tilde{\mathbf{g}}^{\ell+1} \otimes \tilde{\mathbf{h}}^{\ell+1}), 1 \right\}. \end{aligned} \quad (\text{A.7})$$

In our numerical experiments conducted in Section 5, we always adopt the iterative scheme (A.7) since the proximal parameter  $\varepsilon$  in our iEPPA does not need to take a small value.

## Appendix B Dykstra's algorithm with Kullback-Leibler projections

The Dykstra's algorithm with Kullback-Leibler projections (DyKL) [5] is adapted in [6] to solve the following entropic regularized capacity constrained optimal transport problem:

$$\begin{aligned} \min_{X \in \mathbb{R}^{m \times n}} \langle C, X \rangle + \varepsilon \sum_{s=1}^m \sum_{r=1}^n X_{rs} (\log X_{rs} - 1) \\ \text{s.t.} \quad X \mathbf{1}_n = \mathbf{a}, \quad X^\top \mathbf{1}_m = \mathbf{b}, \quad 0 \leq X \leq U, \end{aligned} \quad (\text{B.1})$$

where  $C \in \mathbb{R}_+^{m \times n}$ ,  $U \in \mathbb{R}_{++}^{m \times n}$ ,  $\mathbf{a} := (a_1, \dots, a_m)^\top \in \Sigma_m$ ,  $\mathbf{b} := (b_1, \dots, b_n)^\top \in \Sigma_n$ . Recall the definition of the Kullback-Leibler (KL) divergence between  $X \in \mathbb{R}_+^{m \times n}$  and  $Y \in \mathbb{R}_{++}^{m \times n}$  is given as follows:

$$\mathbf{KL}(X, Y) = \sum_{r,s} (x_{rs} \log(x_{rs}/y_{rs}) - x_{rs} + y_{rs}).$$

Moreover, given a convex set  $\mathcal{S} \subseteq \mathbb{R}_+^{m \times n}$  and  $Y \in \mathbb{R}_{++}^{m \times n}$ , the projection associated with the KL divergence (called KL projection) is defined as  $\text{Proj}_{\mathcal{S}}^{\mathbf{KL}}(Y) := \arg \min_{X \in \mathcal{S}} \mathbf{KL}(X, Y)$ . Thus, problem (B.1) can be equivalently reformulated as

$$\min_{X \in \mathbb{R}^{m \times n}} \mathbf{KL}(X, K) \quad \text{s.t.} \quad X \in \mathcal{S}_1 \cap \mathcal{S}_2 \cap \mathcal{S}_3,$$

where  $K := e^{-C/\varepsilon}$  is the kernel matrix,  $\mathcal{S}_1 := \{X \in \mathbb{R}^{m \times n} : X \mathbf{1}_n = \mathbf{a}\}$ ,  $\mathcal{S}_2 := \{X \in \mathbb{R}^{m \times n} : X^\top \mathbf{1}_m = \mathbf{b}\}$  and  $\mathcal{S}_3 := \{X \in \mathbb{R}^{m \times n} : X \leq U\}$ . Then, the DyKL is presented as follows: let  $X^0 = K$ ,  $Q_1^0 = Q_2^0 = Q_3^0 = \mathbf{1}_m \mathbf{1}_n^\top$ , then for  $k \geq 0$ , compute

$$\begin{aligned} \Pi_0^{k+1} &= X^k, \\ \Pi_1^{k+1} &= \text{Proj}_{\mathcal{S}_1}^{\text{KL}}(\Pi_0^{k+1} \circ Q_1^k), \quad Q_1^{k+1} = Q_1^k \circ (\Pi_0^{k+1} ./ \Pi_1^{k+1}), \\ \Pi_2^{k+1} &= \text{Proj}_{\mathcal{S}_2}^{\text{KL}}(\Pi_1^{k+1} \circ Q_2^k), \quad Q_2^{k+1} = Q_2^k \circ (\Pi_1^{k+1} ./ \Pi_2^{k+1}), \\ \Pi_3^{k+1} &= \text{Proj}_{\mathcal{S}_3}^{\text{KL}}(\Pi_2^{k+1} \circ Q_3^k), \quad Q_3^{k+1} = Q_3^k \circ (\Pi_2^{k+1} ./ \Pi_3^{k+1}), \\ X^{k+1} &= \Pi_3^{k+1}, \end{aligned} \tag{B.2}$$

where  $\circ$  denotes the Hadamard product. Note that the above iterative scheme is a slightly different but an equivalent form of the DyKL used in [6]. We adapt it here because it is more explicit and convenient for comparison. Moreover, by simple calculations, one can verify that

$$\begin{aligned} \Pi_1^{k+1} &= \text{Proj}_{\mathcal{S}_1}^{\text{KL}}(\Pi_0^{k+1} \circ Q_1^k) = \text{Diag}\left(\mathbf{a} ./ ((\Pi_0^{k+1} \circ Q_1^k) \mathbf{1}_n)\right) (\Pi_0^{k+1} \circ Q_1^k), \\ \Pi_2^{k+1} &= \text{Proj}_{\mathcal{S}_2}^{\text{KL}}(\Pi_1^{k+1} \circ Q_2^k) = (\Pi_1^{k+1} \circ Q_2^k) \text{Diag}\left(\mathbf{b} ./ ((\Pi_1^{k+1} \circ Q_2^k)^\top \mathbf{1}_m)\right), \\ \Pi_3^{k+1} &= \text{Proj}_{\mathcal{S}_3}^{\text{KL}}(\Pi_2^{k+1} \circ Q_3^k) = \min\{\Pi_2^{k+1} \circ Q_3^k, U\}. \end{aligned}$$

It is worth noting that the DyKL in (B.2) may suffer from severe numerical issues when  $\varepsilon$  takes a small value. Thus, one may need to carry out the computations of  $\Pi_i^k$  and  $Q_i^k$  ( $i = 1, 2, 3$ ) in the log domain to alleviate the numerical instability. Specifically, by taking logarithm on both sides of above equations and letting  $\tilde{X}^k := \varepsilon \log X^k$ ,  $\tilde{\Pi}_i^k := \varepsilon \log \Pi_i^k$ ,  $\tilde{Q}_i^k := \varepsilon \log Q_i^k$ ,  $\tilde{\mathbf{a}} := \varepsilon \log \mathbf{a}$ ,  $\tilde{U} := \varepsilon \log U$ , we obtain after some manipulations that

$$\begin{aligned} \tilde{\Pi}_0^{k+1} &= \tilde{X}^k, \\ \tilde{\Pi}_1^{k+1} &= \left[ \tilde{\mathbf{a}} - \varepsilon \log \left( \left[ \exp((\tilde{\Pi}_0^{k+1} + \tilde{Q}_1^k) / \varepsilon) \right] \mathbf{1}_n \right) \right] \mathbf{1}_n^\top + \tilde{\Pi}_0^{k+1} + \tilde{Q}_1^k, \quad \tilde{Q}_1^{k+1} = \tilde{Q}_1^k + \tilde{\Pi}_0^{k+1} - \tilde{\Pi}_1^{k+1}, \\ \tilde{\Pi}_2^{k+1} &= \mathbf{1}_m \left[ \tilde{\mathbf{b}} - \varepsilon \log \left( \left[ \exp((\tilde{\Pi}_1^{k+1} + \tilde{Q}_2^k) / \varepsilon) \right]^\top \mathbf{1}_m \right) \right]^\top + \tilde{\Pi}_1^{k+1} + \tilde{Q}_2^k, \quad \tilde{Q}_2^{k+1} = \tilde{Q}_2^k + \tilde{\Pi}_1^{k+1} - \tilde{\Pi}_2^{k+1}, \\ \tilde{\Pi}_3^{k+1} &= \min\{\tilde{\Pi}_2^{k+1} + \tilde{Q}_3^k, \tilde{U}\}, \quad \tilde{Q}_3^{k+1} = \tilde{Q}_3^k + \tilde{\Pi}_2^{k+1} - \tilde{\Pi}_3^{k+1}, \\ \tilde{X}^{k+1} &= \tilde{\Pi}_3^{k+1}. \end{aligned} \tag{B.3}$$

In this stabilization framework, the initialization is set to  $\tilde{X}^0 = -C$  and  $\tilde{Q}_1^0 = \tilde{Q}_2^0 = \tilde{Q}_3^0 = 0$ . When checking the primal feasibility accuracy, we recover  $X^{k+1}$  by setting  $X^{k+1} = \exp(\tilde{X}^{k+1} / \varepsilon)$ .

## Appendix C Construction of a tomographic projection along a given direction

Let  $p$  be a nonnegative integer. We consider the following four directions

$$\vec{v} = (1, p), (1, -p), (p, 1) \text{ and } (p, -1).$$

Note that when  $p \in \{0, 1\}$ , we only have two directions. The process to find the projection  $\mathcal{A}^{(i)}(X)$  along a given direction  $\vec{v}$  is described as follows (see Figure 8 for a concrete example):

1. Plot the entries of  $X$  as points on the integer grid  $\{1, \dots, n\} \times \{1, \dots, n\}$ .
2. For each point, draw a line  $v_j$  which is parallel to  $\vec{v}$ , identify all other points for which  $v_j$  passes through.
3. Take the sum of the entries of  $X$  for all points on  $v_j$  to define  $(\mathcal{A}^{(i)}(X))_j$ .

- Repeat this process until all  $\{v_j\}$  covers the whole grid, i.e., covers all entries of  $X$ .

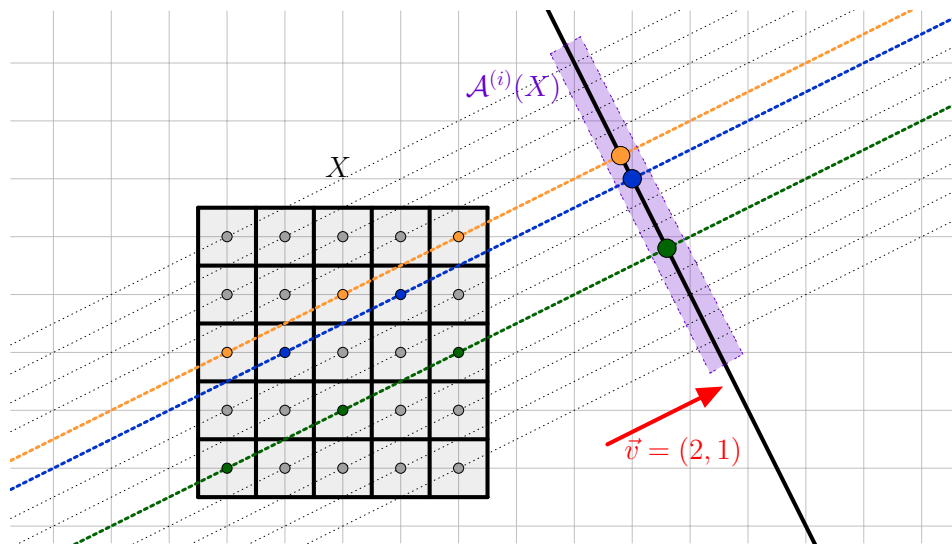


Figure 8: Construction of the projection operator along  $\vec{v} = (2, 1)$  for a  $5 \times 5$  matrix  $X$ .

## References

- [1] Isabelle Abraham, Romain Abraham, Maitine Bergounioux, and Guillaume Carlier. Tomographic reconstruction from a few views: a multi-marginal optimal transport approach. *Applied Mathematics and Optimization*, 75(1):55–73, 2017.
- [2] J. Altschuler, J. Weed, and P. Rigollet. Near-linear time approximation algorithms for optimal transport via Sinkhorn iteration. In *Advances in neural information processing systems*, pages 1964–1974, 2017.
- [3] A. Auslender and M. Haddou. An interior-proximal method for convex linearly constrained problems and its extension to variational inequalities. *Mathematical Programming*, 71(1):77–100, 1995.
- [4] H.H. Bauschke and J.M. Borwein. Legendre functions and the method of random Bregman projections. *Journal of Convex Analysis*, 4(1):27–67, 1997.
- [5] H.H. Bauschke and A.S. Lewis. Dykstras algorithm with Bregman projections: A convergence proof. *Optimization*, 48(4):409–427, 2000.
- [6] J.-D. Benamou, G. Carlier, M. Cuturi, L. Nenna, and G. Peyré. Iterative Bregman projections for regularized transportation problems. *SIAM Journal on Scientific Computing*, 37(2):A1111–A1138, 2015.
- [7] Maitine Bergounioux, Isabelle Abraham, Romain Abraham, Guillaume Carlier, Erwan Le Pennec, and Emmanuel Trélat. Variational methods for tomographic reconstruction with few views. *Milan Journal of Mathematics*, 86(2):157–200, 2018.
- [8] L.M. Bregman. The relaxation method of finding the common point of convex sets and its application to the solution of problems in convex programming. *USSR Computational Mathematics and Mathematical Physics*, 7(3):200–217, 1967.
- [9] Y. Censor and A. Lent. An iterative row-action method for interval convex programming. *Journal of Optimization theory and Applications*, 34(3):321–353, 1981.

- [10] Y. Censor and S.A. Zenios. Proximal minimization algorithm with  $D$ -functions. *Journal of Optimization Theory and Applications*, 73(3):451–464, 1992.
- [11] G. Chen and M. Teboulle. Convergence analysis of a proximal-like minimization algorithm using Bregman functions. *SIAM Journal on Optimization*, 3(3):538–543, 1993.
- [12] M. Cuturi. Sinkhorn distances: Lightspeed computation of optimal transport. In *Advances in Neural Information Processing Systems*, pages 2292–2300, 2013.
- [13] R.L. Dykstra. An algorithm for restricted least squares regression. *Journal of the American Statistical Association*, 78(384):837–842, 1983.
- [14] J. Eckstein. Nonlinear proximal point algorithms using Bregman functions, with applications to convex programming. *Mathematics of Operations Research*, 18(1):202–226, 1993.
- [15] J. Eckstein. Approximate iterations in Bregman-function-based proximal algorithms. *Mathematical Programming*, 83(1-3):113–123, 1998.
- [16] P.P.B Eggermont. Multiplicative iterative algorithms for convex programming. *Linear Algebra and its Applications*, 130:25–42, 1990.
- [17] A. Grandy and L. Veraart. Bayesian methodology for systemic risk assessment in financial networks. *Management Science*, 63:3999–4446, 2017.
- [18] A.J. Hoffman. On approximate solutions of systems of linear inequalities. *Journal of Research of the National Bureau of Standards*, 49(4):263–265, 1952.
- [19] V. Holy and K. Safr. Disaggregating input-output tables by the multidimensional RAS method. *arXiv preprint arXiv:1704.07814v2*, 2019.
- [20] A.N. Iusem, B.F. Svaiter, and M. Teboulle. Entropy-like proximal methods in convex programming. *Mathematics of Operations Research*, 19(4):790–814, 1994.
- [21] A.N. Iusem and M. Teboulle. Convergence rate analysis of nonquadratic proximal methods for convex and linear programming. *Mathematics of Operations Research*, 20(3):657–677, 1995.
- [22] J. Korman and R.J. McCann. Insights into capacity-constrained optimal transport. *Proceedings of the National Academy of Sciences*, 110(25):10064–10067, 2013.
- [23] J. Korman and R.J. McCann. Optimal transportation with capacity constraints. *Transactions of the American Mathematical Society*, 367(3):1501–1521, 2015.
- [24] V.L. Levin. The problem of mass transfer in a topological space and probability measures with given marginal measures on the product of two spaces. *Doklady Akademii Nauk SSSR*, 276(5):1059–1064, 1984.
- [25] Z.-Q. Luo and P. Tseng. On the convergence of the coordinate descent method for convex differentiable minimization. *Journal of Optimization Theory and Applications*, 72(1):7–35, 1992.
- [26] Z.-Q. Luo and P. Tseng. On the convergence rate of dual ascent methods for linearly constrained convex minimization. *Mathematics of Operations Research*, 18(4):846–867, 1993.
- [27] J. Nocedal and S. Wright. *Numerical Optimization*. Springer Science and Business Media, 2006.
- [28] G. Peyré and M. Cuturi. Computational optimal transport. *Foundations and Trends® in Machine Learning*, 11(5-6):355–607, 2019.
- [29] B. T. Polyak. *Introduction to optimization*. Optimization Software Inc., New York, 1987.

- [30] R. T. Rockafellar. *Convex Analysis*. Princeton University Press, Princeton, 1970.
- [31] R. T. Rockafellar and R. J-B. Wets. *Variational Analysis*. Springer, 1998.
- [32] A. Ruszczyński. *Nonlinear Optimization*. Princeton University Press, Princeton, 2006.
- [33] R. Sinkhorn. Diagonal equivalence to matrices with prescribed row and column sums. *The American Mathematical Monthly*, 74(4):402–405, 1967.
- [34] M. Teboulle. Entropic proximal mappings with applications to nonlinear programming. *Mathematics of Operations Research*, 17(3):670–690, 1992.
- [35] M. Teboulle. Convergence of proximal-like algorithms. *SIAM Journal on Optimization*, 7(4):1069–1083, 1997.
- [36] R.J. Tibshirani. Dykstra’s algorithm, ADMM, and coordinate descent: Connections, insights, and extensions. In *Advances in Neural Information Processing Systems*, pages 517–528, 2017.
- [37] P. Tseng. Dual coordinate ascent methods for non-strictly convex minimization. *Mathematical Programming*, 59(1-3):231–247, 1993.
- [38] S. Weber, C. Schnörr, T. Schüle, and J. Hornegger. Binary tomography by iterating linear programs. In *Geometric Properties for Incomplete Data*, pages 183–197, 2006.
- [39] Y. Xie, X. Wang, R. Wang, and H. Zha. A fast proximal point method for computing exact Wasserstein distance. In *Proceedings of the 35th Uncertainty in Artificial Intelligence Conference*, pages 433–453, 2020.